

PRECONDITIONED NONSYMMETRIC/SYMMETRIC DISCONTINUOUS GALERKIN METHOD FOR ELLIPTIC PROBLEM WITH RECONSTRUCTED DISCONTINUOUS APPROXIMATION

RUO LI, QICHENG LIU, AND FANYI YANG

ABSTRACT. In this paper, we propose and analyze an efficient preconditioning method for the elliptic problem based on the reconstructed discontinuous approximation method. This method is originally proposed in [Li et al., J. Sci. Comput. 80(1), 2019] that an arbitrarily high-order approximation space with one unknown per element is reconstructed by solving a local least squares fitting problem. This space can be directly used with the symmetric/nonsymmetric interior penalty discontinuous Galerkin methods. The least squares problem is modified in this paper, which allows us to establish a norm equivalence result between the reconstructed high-order space and the piecewise constant space. This property further inspires us to construct a preconditioner from the piecewise constant space. The preconditioner is shown to be optimal that the upper bound of the condition number to the preconditioned symmetric/nonsymmetric system is independent of the mesh size. In addition, we can enjoy the advantage on the efficiency of the approximation in number of degrees of freedom compared with the standard DG method. Numerical experiments are provided to demonstrate the validity of the theory and the efficiency of the proposed method.

keywords: discontinuous Galerkin method; reconstructed discontinuous approximation; symmetric/nonsymmetric interior penalty method; preconditioning; least squares fitting;

1. INTRODUCTION

In recent years, there have been extensive studies focused on the development of discontinuous Galerkin (DG) methods, and now DG methods are the very standard numerical methods in solving a variety of partial differential equations; we refer to [13, 17, 39] for some monographs. The DG methods use totally discontinuous piecewise polynomial approximation space, which gives several advantages over other types of finite element methods [6]. The full discontinuity across the element faces brings the advantage of the flexibility on the mesh partition. The DG methods can be easily applied to the polygonal mesh and the mesh with hanging nodes, see [14, 13, 34] for some examples. Such meshes ease the triangulation of complex geometries and curved boundaries. The implementation of the DG space is easy because the basis functions are entirely local. On the other hand, the DG method may be computationally expensive and inefficient on the approximation because of the significant increase in the number of degrees of freedom [25]. This shortcoming is remarkable especially for the high-order scheme. In addition, the final linear system is ill-conditioned with the condition number grows like $O(h^{-2})$ [15].

To overcome the issue on the huge number of degrees of freedom, we proposed a reconstructed discontinuous approximation method, where a high-order approximation space is constructed with only one unknown per element [29]. The main step of the reconstruction is solving a local least squares fitting problem on the element patch. This space is a small subspace of the standard discontinuous piecewise polynomial space, and inherits the flexibility on the mesh partition. We prove the optimal approximation estimate, while the number of degrees of freedom is substantially reduced to the number of elements in the mesh. This approach has been successfully applied to a series of classical problems [28, 31, 32, 27, 33]. In this paper, we modify the local least squares problem in [29] by adding a constraint at the barycenter. This modification essentially brings us the non-degeneracy to the reconstruction operator, which allows us to further develop an efficient preconditioner based on the piecewise constant space. In solving the elliptic problem with the reconstructed space, the first conclusion from this property is the $O(h^{-2})$ condition number estimate, which is the same as the standard DG method.

Solving the resulting linear system efficiently is of special concern in finite element methods, and the most common method is to construct a proper preconditioner that can significantly reduce the condition number in the preconditioned system. The Schwarz method is one of the popular methods for preconditioning the linear system arising from the DG discretization. In [23, 1, 3, 2, 9, 26], a wide class of overlapping and non-overlapping domain decomposition methods are proposed and analyzed. The condition number of the preconditioned linear system has the bounds $O(H/\delta)$ and $O(H/h)$, where H, h and δ stand for the granularity of the coarse and fine grids and the size of the overlap, respectively.

In addition, there are other kinds of preconditioners based on the additive Schwarz framework designed for DG methods, like balancing domain decomposition methods, balancing domain decomposition with constraints and the auxiliary space methods, see e.g. [20, 19, 18, 12, 6]. Multigrid methods are also the widely used approaches to design preconditioners for the DG discretization. The main idea behind these methods is to correct the error after a few smoothing iterations on a coarser grid [43]. We refer to [24, 4, 11] for geometrical multigrid methods and [35, 5] for algebraic multigrid methods.

In this paper, we construct and analyze an efficient preconditioning method for the reconstructed space in solving the elliptic system. We first employ the symmetric/nonsymmetric interior penalty DG method in the numerical scheme. The error estimates under error measurements are standard under the Lax-Milgram framework. The main feature of the proposed scheme is that only one degree of freedom is involved per element, which first gives a higher efficiency on the finite element approximation in number of degrees of freedom. We conduct a series of numerical tests to show that our method can use much fewer degrees of freedom to achieve the comparable numerical error. Second, the size of the reconstructed space is always the same as the piecewise constant space. From this fact, we can construct a preconditioner from the piecewise constant space to any high-order reconstructed space. The low-order preconditioning is also a classical technique in finite element methods for preconditioning the high-order discretization, see [16, 37, 36]. In our method, the modified local least squares problem enables us to prove a norm equivalence between the piecewise constant space and the high-order reconstructed space on the same mesh. This crucial property further allows us to prove that the preconditioner is optimal for any high-order accuracy in the sense that the upper bound of the condition number to the preconditioned system is independent of the mesh size. A series of numerical experiments including an example on the polygonal mesh are presented to demonstrate the efficiency of the preconditioner in two and three dimensions.

The rest of this paper is organized as follows. In Section 2, we introduce the notation and recall some inequalities. Section 3 introduces the reconstructed discontinuous approximation method including the construction to the reconstruction operator and some basic properties of the space. Section 4 presents the symmetric/nonsymmetric interior penalty DG methods with the reconstructed space to the elliptic problem. The preconditioning method is also given in this section. In Section 5, the accuracy and the efficiency of the proposed method are illustrated by a series of numerical tests. A brief conclusion is given in Section 6.

2. PRELIMINARIES

Let $\Omega \subset \mathbb{R}^d (d = 2, 3)$ be a bounded convex polygonal (polyhedral) domain with the boundary $\partial\Omega$. We denote by \mathcal{T}_h a quasi-uniform triangulation over the domain Ω . Let \mathcal{E}_h^I and \mathcal{E}_h^B be the collections of all $d - 1$ dimensional interior faces in the partition \mathcal{T}_h , and faces lying on the boundary $\partial\Omega$, respectively. We further set $\mathcal{E}_h := \mathcal{E}_h^I \cup \mathcal{E}_h^B$ as the set of all faces. For any element $K \in \mathcal{T}_h$ and any face $e \in \mathcal{E}_h$, we set $h_K := \text{diam}(K)$ and $h_e := \text{diam}(e)$ as their diameters, and we let ρ_K be the radius of the largest inscribed disk (ball) in K . We denote by $h := \max_{K \in \mathcal{T}_h} h_K$ the mesh size to \mathcal{T}_h , and by $\rho := \min_{K \in \mathcal{T}_h} \rho_K$. The mesh \mathcal{T}_h is assumed to be quasi-uniform in the sense that there exists a constant $C_\sigma > 0$ such that $h \leq C_\sigma \rho$.

The quasi-uniformity of \mathcal{T}_h brings us the following fundamental estimates: the trace estimate and the inverse estimate: there exist constants C independent of h such that

$$(1) \quad \|v\|_{L^2(\partial K)}^2 \leq C(h_K^{-1}\|v\|_{L^2(K)}^2 + h_K\|v\|_{H^1(K)}^2), \quad \forall v \in H^1(K), \quad \forall K \in \mathcal{T}_h,$$

$$(2) \quad \|v\|_{H^q(K)} \leq Ch_K^{p-q}\|v\|_{H^p(K)}, \quad q \geq p \geq 0, \quad \forall v \in \mathbb{P}_m(K), \quad \forall K \in \mathcal{T}_h,$$

where $\mathbb{P}_m(\cdot)$ denotes the space of polynomials of degree less than m .

Next, we introduce the following trace operators associated with the weak forms, which are commonly used in the DG framework. Let $e \in \mathcal{E}_h^I$ be any interior face shared by two elements K^+ and K^- with the unit outward normal vectors \mathbf{n}^+ and \mathbf{n}^- along e , respectively. For any piecewise smooth scalar-valued function v and vector-valued function $\boldsymbol{\tau}$, the jump operator $[\cdot]$ and the average operator $\{\cdot\}$ are defined as

$$\begin{aligned} [v]|_e &:= v^+|_e \mathbf{n}^+ + v^-|_e \mathbf{n}^-, & \{v\}|_e &:= \frac{1}{2}(v^+|_e + v^-|_e), \\ [\boldsymbol{\tau}]|_e &:= \boldsymbol{\tau}^+|_e \cdot \mathbf{n}^+ + \boldsymbol{\tau}^-|_e \cdot \mathbf{n}^-, & \{\boldsymbol{\tau}\}|_e &:= \frac{1}{2}(\boldsymbol{\tau}^+|_e + \boldsymbol{\tau}^-|_e), \end{aligned} \quad \forall e \in \mathcal{E}_h^I,$$

where $v^\pm := v|_{K^\pm}$, $\boldsymbol{\tau}^\pm := \boldsymbol{\tau}|_{K^\pm}$. For any boundary face $e \in \mathcal{E}_h^B$, the trace operators are modified as

$$[v]|_e := v|_e \mathbf{n}, \quad \{v\}|_e := v|_e, \quad [\boldsymbol{\tau}]|_e := \boldsymbol{\tau}|_e \cdot \mathbf{n}, \quad \{\boldsymbol{\tau}\}|_e := \boldsymbol{\tau}|_e, \quad \forall e \in \mathcal{E}_h^B,$$

where \mathbf{n} is the unit outward normal to e .

For a bounded domain D , $L^2(D)$ and $H^r(D)$ denote the usual Sobolev spaces with the exponent $r \geq 0$, and we also follow their associated inner products, seminorms and norms. Throughout this paper, C and C with subscripts are denoted to be generic constants that may vary in different occurrences but are always independent of the mesh size h . We also point out that these constants may depend on the polynomial degree, the quasi-uniformity measure C_σ and the coefficient in the problem (3), such as the constants appearing in the trace and inverse estimates (1) - (2). We refer to [13] for more details about the constants in (1) - (2).

In this paper, we are concerned with the elliptic problem defined on Ω , which seeks u such that

$$(3) \quad \begin{aligned} -\nabla \cdot (A\nabla u) &= f, & \text{in } \Omega, \\ u &= g, & \text{on } \partial\Omega, \end{aligned}$$

where $f \in L^2(\Omega)$ is a given source function and $g \in H^{3/2}(\partial\Omega)$ is the boundary condition. The coefficient $A \in \mathbb{R}^{d \times d}$ is assumed to be a symmetric positive definite matrix. By the elliptic regularity theory, the problem (3) admits a unique solution in $H^2(\Omega)$. We are aiming to give a preconditioned interior penalty discontinuous Galerkin method for the problem (3), based on a reconstructed approximation space.

3. THE RECONSTRUCTED DISCONTINUOUS APPROXIMATION METHOD

In this section, we will introduce a linear reconstruction operator to obtain a discontinuous approximation space for the given mesh \mathcal{T}_h . The reconstructed space can achieve a high-order accuracy while the number of degrees of freedom always remain the same as the number of elements in \mathcal{T}_h . The construction of the operator includes two steps.

Step 1. For each $K \in \mathcal{T}_h$, we construct an element patch $S(K)$, which consists of K itself and some surrounding elements. The size of the patch is controlled with a given threshold $\#S$. The construction of the element patch $S(K)$ is conducted by a recursive algorithm. We begin by setting $S_0(K) = \{K\}$, and define $S_t(K)$ recursively:

$$(4) \quad S_t(K) = \bigcup_{K' \in S_{t-1}(K)} \bigcup_{K'' \in \Delta(K')} K'', \quad t = 0, 1, \dots$$

where $\Delta(K) := \{K' \in \mathcal{T}_h \mid \overline{K} \cap \overline{K'} \neq \emptyset\}$. The recursion stops once t meets the condition that the cardinality $\#S_t(K) \geq \#S$, and we let the patch $S(K) := S_t(K)$. Applying the recursive algorithm (4) to all elements in \mathcal{T}_h , each $K \in \mathcal{T}_h$ has a large element patch $S(K)$.

Step 2. For each $K \in \mathcal{T}_h$, we solve a local least squares fitting problem on the patch $S(K)$. We let \mathbf{x}_K be the barycenter of the element K and mark barycenters of all elements as collocation points. Let $I(K)$ be the set of collocation points located inside the domain of $S(K)$,

$$I(K) := \{\mathbf{x}_{K'} \mid K' \in S(K)\},$$

Let U_h^0 be the piecewise constant space with respect to \mathcal{T}_h ,

$$U_h^0 := \{v_h \in L^2(\Omega) \mid v_h|_K \in \mathbb{P}_0(K), \forall K \in \mathcal{T}_h\}.$$

Given a piecewise constant function $v_h \in U_h^0$, for each $K \in \mathcal{T}_h$, we seek a polynomial of degree m ($m \geq 1$) by the following constrained local least squares problem on the patch $S(K)$,

$$(5) \quad \begin{aligned} \arg \min_{p \in \mathbb{P}_m(S(K))} \sum_{\mathbf{x} \in I(K)} (p(\mathbf{x}) - v_h(\mathbf{x}))^2, \\ \text{s.t. } p(\mathbf{x}_K) = v_h(\mathbf{x}_K). \end{aligned}$$

We note that the unsolvence of the problem (5) depends on the distribution of collocation points in $I(K)$. We make the following assumption of $S(K)$ and $I(K)$.

Assumption 1. For any element $K \in \mathcal{T}_h$ and any polynomial $p \in \mathbb{P}_m(S(K))$, $p|_{I(K)} = 0$ implies $p|_{S(K)} = 0$.

Assumption 1 indicates that the points in $I(K)$ deviate from being located on an algebraic curve (surface) of degree m . In addition, Assumption 1 implies the condition $\#I(K) = \#S(K) \geq \dim(\mathbb{P}_m(\cdot))$. The existence and the uniqueness of the solution to (5) are stated in the following lemma.

Lemma 1. For each $K \in \mathcal{T}_h$, the problem (5) admits a unique solution.

Proof. We mainly prove the uniqueness of the solution since the existence is trivial. Let p_1 and p_2 be the solutions to (5). Let $q \in \mathbb{P}_m(S(K))$ be any polynomial such that $q(\mathbf{x}_K) = 0$, and let $t > 0$ be arbitrary. For $i = 1, 2$, $p_i + tq$ satisfies the constraint in (5). Bringing $p_i + tq$ into (5) yields that

$$\sum_{\mathbf{x} \in I(K)} (p_i(\mathbf{x}) + tq(\mathbf{x}) - v_h(\mathbf{x}))^2 \geq \sum_{\mathbf{x} \in I(K)} (p_i(\mathbf{x}) - v_h(\mathbf{x}))^2,$$

which further gives

$$\sum_{\mathbf{x} \in I(K)} -2tq(\mathbf{x})(p_i(\mathbf{x}) - v_h(\mathbf{x})) + t^2(q(\mathbf{x}))^2 \geq 0.$$

Because q and t are arbitrary, the above inequality gives us that

$$(6) \quad \sum_{\mathbf{x} \in I(K)} q(\mathbf{x})(p_i(\mathbf{x}) - v_h(\mathbf{x})) = 0 \quad \text{and} \quad \sum_{\mathbf{x} \in I(K)} q(\mathbf{x})(p_1(\mathbf{x}) - p_2(\mathbf{x})) = 0.$$

Note that $(p_1 - p_2) \in \mathbb{P}_m(S(K))$ with $(p_1 - p_2)(\mathbf{x}_K) = 0$. Letting $q = p_1 - p_2$ immediately shows that $p_1 - p_2$ vanishes at all points in $I(K)$. By Assumption 1, we know that $p_1 - p_2 = 0$. This completes the proof. \square

We denote by $v_{h,S(K)} \in \mathbb{P}_m(S(K))$ the solution to (5). From the proof of Lemma 1, it can be seen that $v_{h,S(K)}$ linearly depends on the given function v_h , which allows us to define a local linear operator $\mathcal{R}_K^m : U_h^0 \rightarrow \mathbb{P}_m(S(K))$ such that $\mathcal{R}_K^m v_h$ is the solution $v_{h,S(K)}$ of the problem (5) for $\forall v_h \in U_h^0$.

Further, we define a global reconstruction operator \mathcal{R}^m in an element-wise manner, which reads

$$(7) \quad \begin{aligned} \mathcal{R}^m : U_h^0 &\longrightarrow U_h^m, \\ v_h &\longrightarrow \mathcal{R}^m v_h, \end{aligned} \quad (\mathcal{R}^m v_h)|_K := (\mathcal{R}_K^m v_h)|_K, \quad \forall K \in \mathcal{T}_h.$$

For any element $K \in \mathcal{T}_h$, $(\mathcal{R}^m v_h)|_K$ is the restriction of $\mathcal{R}_K^m v_h$ on K . Thus, $(\mathcal{R}^m v_h)|_K$ has the same expression as $\mathcal{R}_K^m v_h$. By \mathcal{R}^m , any piecewise constant function v_h is mapped into a piecewise m -th degree polynomial function $\mathcal{R}^m v_h$. Here $U_h^m := \mathcal{R}^m U_h^0$ is defined as the image space, which is actually the approximation space in the numerical scheme. From the linearity of \mathcal{R}^m , we know that $\text{rank}(\mathcal{R}^m) \leq \dim(U_h^0)$. In fact, we can prove that \mathcal{R}^m is non-degenerate.

Lemma 2. *The operator \mathcal{R}^m is full-rank, i.e. $\dim(U_h^m) = \dim(U_h^0)$.*

Proof. Since \mathcal{R}^m is linear, it is equivalent to show that if some $v_h \in U_h^0$ satisfy that $\mathcal{R}^m v_h = 0$, then $v_h = 0$. For such v_h , the constraint in (5) indicates that $v_h(\mathbf{x}_K) = (\mathcal{R}^m v_h)(\mathbf{x}_K) = 0$ for every element $K \in \mathcal{T}_h$. Then, we conclude that v_h must be the zero function, which completes the proof. \square

We note that Lemma 2 is essentially established on the constraint in (5), which is the major improvement compared with our previous methods in [30, 29]. This constraint and the non-degenerate property are also fundamental for us to develop an efficient preconditioning method based on the space U_h^0 .

Let us give a group of basis functions to the reconstructed space U_h^m . We denote by n_e the number of elements in \mathcal{T}_h , and there holds $\dim(U_h^m) = n_e$. For an element $K \in \mathcal{T}_h$ numbered by the index i , we associate K with a piecewise constant function $e_i \in U_h^0$ such that

$$(8) \quad e_i(\mathbf{x}) = \begin{cases} 1, & \mathbf{x} \in K, \\ 0, & \text{otherwise.} \end{cases}$$

Let $\lambda_j := \mathcal{R}^m e_j$ ($1 \leq j \leq n_e$). Then, we claim that $\{\lambda_j\}_{j=1}^{n_e}$ are linearly independent. Again from the constraint in (5), we know that $\lambda_j(\mathbf{x}_K) = 1$ with K indexed by j , and λ_j vanishes at other collocation points. Consider the group of coefficients $\{a_j\}_{j=1}^{n_e}$ such that

$$(9) \quad a_1 \lambda_1(\mathbf{x}) + a_2 \lambda_2(\mathbf{x}) + \dots + a_{n_e} \lambda_{n_e}(\mathbf{x}) = 0.$$

We let $\mathbf{x} = \mathbf{x}_K$ for each $K \in \mathcal{T}_h$ in (9), and we can know that all $a_j = 0$. The linear independence of $\{\lambda_j\}_{j=1}^{n_e}$ is reached. Since $\lambda_j \in U_h^m$ for $1 \leq j \leq n_e$, we conclude that $U_h^m = \text{span}(\{\lambda_j\}_{j=1}^{n_e})$. Equivalently, $\{\lambda_j\}_{j=1}^{n_e}$ are basis functions of U_h^m . In (8), for any element K' such that $K \notin S(K')$, there holds $e_i|_{S(K')} = 0$, and we can know that $\mathcal{R}_{K'}^m e_i = 0$. This fact implies that λ_i has a compact support that $\text{supp}(\lambda_i) = \bigcup_{K' | K \in S(K')} \overline{K'}$.

Next, we extend the operator \mathcal{R}^m to C^0 smooth functions in a natural way. Given any $v \in C^0(\Omega)$, we define an associated piecewise constant function $\tilde{v}_h \in U_h^0$ such that $\tilde{v}_h = v$ at all collocation points, i.e. $\tilde{v}_h(\mathbf{x}_K) = v(\mathbf{x}_K)$ ($\forall K \in \mathcal{T}_h$). Then $\mathcal{R}^m v$ is defined as $\mathcal{R}^m v := \mathcal{R}^m \tilde{v}_h$. By the basis functions $\{\lambda_j\}_{j=1}^{n_e}$, $\mathcal{R}^m v$ has the expansion that

$$(10) \quad \mathcal{R}^m v = v(\mathbf{x}_{K_1}) \lambda_1 + v(\mathbf{x}_{K_2}) \lambda_2 + \dots + v(\mathbf{x}_{K_{n_e}}) \lambda_{n_e}, \quad \forall v \in C^0(\Omega),$$

where K_j is the element indexed by j .

Remark 1. *The least squares problem (5) does not rely on the geometrical shape of the element. The reconstruction process can be applied to the polygonal mesh. We refer to [10] for the shape regularity conditions, which bring the trace estimate (1) and the inverse estimate (2) for the polygonal mesh. All estimates in this paper can be extended on the shape-regular polygonal mesh without any difficulty.*

We present the following stability property of the reconstruction operator.

Lemma 3. *For any element $K \in \mathcal{T}_h$, there holds*

$$(11) \quad \|\mathcal{R}_K^m g\|_{L^\infty(S(K))} \leq (1 + 2\Lambda(m, K)\sqrt{\#S(K)}) \max_{\mathbf{x} \in I(K)} |g|, \quad \forall g \in C^0(\Omega),$$

where

$$(12) \quad \Lambda(m, K) := \max_{p \in \mathbb{P}_m(S(K))} \frac{\max_{\mathbf{x} \in S(K)} |p(\mathbf{x})|}{\max_{\mathbf{x} \in I(K)} |p(\mathbf{x})|}.$$

Proof. Let $p = \mathcal{R}_K^m g \in \mathbb{P}_m(S(K))$ be the solution to (5) on $S(K)$. By (6), there holds $\sum_{\mathbf{x} \in I(K)} q(\mathbf{x})(p(\mathbf{x}) - g(\mathbf{x})) = 0$ for any $q \in \mathbb{P}_m(S(K))$ with $q(\mathbf{x}_K) = 0$. Setting $q(\mathbf{x}) = p(\mathbf{x}) - g(\mathbf{x}_K)$, we know that $\sum_{\mathbf{x} \in I(K)} (p(\mathbf{x}) - g(\mathbf{x}_K))(p(\mathbf{x}) - g(\mathbf{x})) = 0$. From this equality, we find that

$$\sum_{\mathbf{x} \in I(K)} (p(\mathbf{x}) - g(\mathbf{x}_K))^2 = \sum_{\mathbf{x} \in I(K)} (g - g(\mathbf{x}_K))(p - g(\mathbf{x}_K)).$$

Applying the Cauchy-Schwarz inequality, we have that

$$(13) \quad \sum_{\mathbf{x} \in I(K)} (p - g(\mathbf{x}_K))^2 \leq \sum_{\mathbf{x} \in I(K)} (g - g(\mathbf{x}_K))^2.$$

Combining (13) and the definition (12), we obtain that

$$\begin{aligned} \|p - g(\mathbf{x}_K)\|_{L^\infty(S(K))}^2 &\leq \Lambda(m, K)^2 \max_{\mathbf{x} \in I(K)} (p - g(\mathbf{x}_K))^2 \leq \Lambda(m, K)^2 \sum_{\mathbf{x} \in I(K)} (g - g(\mathbf{x}_K))^2 \\ &\leq 4\Lambda(m, K)^2 \#S(K) \max_{\mathbf{x} \in I(K)} g^2. \end{aligned}$$

Hence, we conclude that

$$\|p\|_{L^\infty(S(K))} \leq \|p - g(\mathbf{x}_K)\|_{L^\infty(S(K))} + |g(\mathbf{x}_K)| \leq (1 + 2\Lambda(m, K)\sqrt{\#S(K)}) \max_{\mathbf{x} \in I(K)} |g|,$$

which completes the proof. \square

We introduce the constants Λ_m and $\bar{\Lambda}_m$ by

$$(14) \quad \Lambda_m := \max_{K \in \mathcal{T}_h} \Lambda(m, K), \quad \bar{\Lambda}_m := \max_{K \in \mathcal{T}_h} (1 + \Lambda_m \sqrt{\#S(K)}).$$

From the stability estimate (11), we have that

$$(15) \quad \|g - \mathcal{R}_K^m g\|_{L^\infty(S(K))} \leq 2\bar{\Lambda}_m \inf_{p \in \mathbb{P}_m(S(K))} \|g - p\|_{L^\infty(S(K))}, \quad \forall g \in C^0(\Omega).$$

The approximation property of \mathcal{R}_K^m can be established on (15).

Lemma 4. *There exists a constant C such that*

$$(16) \quad \|g - \mathcal{R}_K^m g\|_{H^q(K)} \leq C\bar{\Lambda}_m h_K^{m+1-q} \|g\|_{H^{m+1}(S(K))}, \quad 0 \leq q \leq m, \quad \forall K \in \mathcal{T}_h.$$

The proof is quite formal and we refer to [30, Theorem 3.3] for details.

By (15) - (16), the polynomial $\mathcal{R}_K^m g$ has the optimal convergence rate on the element $K \in \mathcal{T}_h$ if $\bar{\Lambda}_m$ admits a uniform upper bound. For each $K \in \mathcal{T}_h$, we let B_{r_K} and B_{R_K} be the largest ball and the smallest ball such that $B_{r_K} \subset \bigcup_{K' \in S(K)} \bar{K}' \subset B_{R_K}$, with the radius r_K and R_K , respectively. By [29, Lemma 5], there holds $\Lambda_m \leq 1 + \varepsilon$ under the condition $r_K \geq m\sqrt{2R_K h_K(1 + 1/\varepsilon)}$. Generally speaking, if the patch $S(K)$ is large enough, there will be $r_K \approx R_K$, and this condition can be then satisfied. Therefore, for this condition we are required to construct a wide element patch to ensure a large r_K . In [29, Lemma 5][30, Lemma 3.4], we prove that this condition can be met when the threshold $\#S$ in (4) is greater than a certain constant, which only depends on m and C_σ . We also notice that this given bound of the size of the patch is usually too large and is impractical in the computer implementation.

As numerical observations, the reconstructed method works very well when the size of the patch is far less than the theoretical value. In Section 5, we list the values $\#S$ in all tests. The threshold is roughly taken as $\#S \approx \frac{d+1}{2} \dim(\mathbb{P}_m(\cdot))$ on quasi-uniform meshes.

Remark 2. For the patch $S(K)$, we consider the special case that the corresponding collocation points set $I(K)$ has exactly $\dim(\mathbb{P}_m(\cdot))$ points, then the solution to the least squares problem (5) becomes the Lagrange interpolation polynomial and the constant $\Lambda(m, K)$ is equal to the Lebesgue constant [38]. To our best knowledge, in two and three dimensions there are few results about the bound of the Lebesgue constant. The Lebesgue constant may grow very fast as h tends to zero, which will hamper the convergence of the scheme. Currently, we can prove that the constant Λ_m admits a uniform upper bound for the wider element patch. The wider element patch will bring more computational cost for filling the stiffness matrix and increase the width of the banded structure, which also leads to more computational cost in the matrix-vector product for our method. This can be regarded as the price we pay for the upper bound to Λ_m . On the other hand, we can give a preconditioning method based on the piecewise constant space for any high-order accuracy, which can be computed efficiently. Consequently, solving the resulting linear system is still observed to be fast in the numerical tests.

Furthermore, the upper bound of $\bar{\Lambda}_m$ certainly depends on the polynomial degree m , and $\bar{\Lambda}_m$ will grow larger as m increases. The precise dependence between $\bar{\Lambda}_m$ and m and the h - m version of the reconstructed space are considered in the future research.

4. APPROXIMATION TO THE ELLIPTIC PROBLEM

In this section, we present the numerical scheme for the elliptic problem (3), based on the interior penalty method and the reconstructed space U_h^m . We seek $u_h \in U_h^m$ such that

$$(17) \quad a_{h,\theta}(u_h, v_h) = l_{h,\theta}(v_h), \quad \forall v_h \in U_h^m,$$

where

$$(18) \quad \begin{aligned} a_{h,\theta}(u_h, v_h) := & \sum_{K \in \mathcal{T}_h} \int_K A \nabla u_h \cdot \nabla v_h \, d\mathbf{x} - \sum_{e \in \mathcal{E}_h} \int_e \{A \nabla u_h\} \cdot [v_h] \, ds \\ & + \theta \sum_{e \in \mathcal{E}_h} \int_e \{A \nabla v_h\} \cdot [u_h] \, ds + \sum_{e \in \mathcal{E}_h} \int_e \mu h_e^{-1} [u_h] [v_h] \, ds, \end{aligned}$$

and

$$l_{h,\theta}(v_h) := \sum_{K \in \mathcal{T}_h} \int_K f_h v_h \, d\mathbf{x} + \theta \sum_{e \in \mathcal{E}_h^B} \int_e g \{A \nabla v_h\} \, ds + \sum_{e \in \mathcal{E}_h^B} \int_e \mu h_e^{-1} g [v_h] \, ds.$$

Here μ is the penalty parameter. We refer to [8, 7] for the derivation of the bilinear form for the interior penalty method. The forms with $\theta = -1/1$ are known as the symmetric/nonsymmetric interior penalty DG methods.

The convergence analysis follows from the standard procedure under the Lax-Milgram framework. Let $U_h := U_h^m + H^2(\Omega)$, and we define the following mesh-dependent energy norms for the error estimation, which read

$$\|v_h\|_{\text{DG}}^2 := \sum_{K \in \mathcal{T}_h} \|\nabla v_h\|_{L^2(K)}^2 + \sum_{e \in \mathcal{E}_h} h_e^{-1} \|[v_h]\|_{L^2(e)}^2, \quad \forall v_h \in U_h,$$

and

$$\|v_h\|_{\text{DG}}^2 := \|v_h\|_{\text{DG}}^2 + \sum_{e \in \mathcal{E}_h} h_e \|\{ \nabla v_h \}\|_{L^2(e)}^2, \quad \forall v_h \in U_h.$$

It is noticeable that both norms are equivalent restricted on the piecewise polynomial space U_h^m , i.e.

$$(19) \quad \|v_h\|_{\text{DG}} \leq \|v_h\|_{\text{DG}} \leq C \|v_h\|_{\text{DG}}, \quad \forall v_h \in U_h^m.$$

The above equivalence estimate follows from the trace estimate (1) and the inverse estimate (2). In addition, from [7, Lemma 2.1], we give the relationship between the energy norm and the L^2 norm, which reads

$$(20) \quad \|v_h\|_{L^2(\Omega)} \leq C \|v_h\|_{\text{DG}} \leq Ch^{-1} \|v_h\|_{L^2(\Omega)}, \quad \forall v_h \in U_h^m.$$

Because the reconstructed space U_h^m is a subspace of the standard discontinuous piecewise polynomial space, the following steps, including the boundedness and the coercivity of $a_{h,\theta}(\cdot, \cdot)$ and the Galerkin orthogonality, can be derived with a standard procedure in the DG framework [8].

Lemma 5. For the symmetric method $\theta = -1$, we let $a_{h,\theta}(\cdot, \cdot)$ be defined with a sufficiently large μ , and for the nonsymmetric method $\theta = 1$, we let $a_{h,\theta}(\cdot, \cdot)$ be defined with any positive $\mu > 0$, there exist constants C such that

$$(21) \quad |a_{h,\theta}(v_h, w_h)| \leq C \|v_h\|_{\text{DG}} \|w_h\|_{\text{DG}}, \quad \forall v_h, w_h \in U_h,$$

$$(22) \quad a_{h,\theta}(v_h, v_h) \geq C \|v_h\|_{\text{DG}}^2, \quad \forall v_h \in U_h^m.$$

We can also share the estimation of the penalty parameter in the symmetric interior penalty DG method, i.e. there exists a threshold $\mu_0(m, C_\sigma, A)$ such that $\mu \geq \mu_0$ yields the coercivity (22). We refer to [21, Remark 12 and Remark 17] for more details on μ_0 , and we also list the choice of μ in numerical tests in Section 5.

Lemma 6. Let $u \in H^2(\Omega)$ be the exact solution to (3), and let $u_h \in U_h^m$ be the numerical solution to (17), there holds

$$(23) \quad a_{h,\theta}(u - u_h, v_h) = 0, \quad \forall v_h \in U_h^m.$$

Combining the approximation result (16) of the space U_h^m and Lemma 5 - Lemma 6 yields the desired error estimation.

Theorem 1. Let $u \in H^{m+1}(\Omega)$ be the exact solution to (3), and let $u_h \in U_h^m$ be the numerical solution to (17), and let the penalty parameter μ be taken as in Lemma 5, there exists a constant C such that

$$(24) \quad \|u - u_h\|_{\text{DG}} \leq C \bar{\Lambda}_m h^m \|u\|_{H^{m+1}(\Omega)}.$$

In addition, for the symmetric method $\theta = -1$, there holds

$$(25) \quad \|u - u_h\|_{L^2(\Omega)} \leq C \bar{\Lambda}_m h^{m+1} \|u\|_{H^{m+1}(\Omega)}.$$

Proof. From Lemma 5 - Lemma 6, one can find that

$$\|u - u_h\|_{\text{DG}} \leq C \|u - v_h\|_{\text{DG}}, \quad \forall v_h \in U_h^m.$$

Let $v_h := \mathcal{R}^m u$. By the approximation property (16) and the trace estimate (1), we have that

$$\|u - v_h\|_{\text{DG}} \leq C \bar{\Lambda}_m h^m \|u\|_{H^{m+1}(\Omega)}.$$

Collecting the above two estimates gives the error estimate (24).

For the symmetric scheme with $\theta = -1$, the L^2 error estimation (25) can be obtained by the standard dual argument, which completes the proof. \square

The error estimates for the nonsymmetric/symmetric interior penalty DG methods have been completed. From Theorem 1, the numerical solution has the optimal convergence rates, as the standard finite element methods. In addition, the proposed method also shares the flexibility in the mesh partition, i.e. the polygonal elements are allowed in the scheme. Since the number of degrees of freedom is fixed as n_e for any $m \geq 1$, one of the advantages is that the scheme with U_h^m will enjoy a better efficiency on the finite element approximation, see Subsection 5.1 for a numerical comparison on the proposed method and the standard DG method.

Next, we focus on the resulting linear system arising in our method. We begin by estimating the condition number. Let $A_{m,\theta}$ be the linear system with respect to the bilinear form $a_{h,\theta}(\cdot, \cdot)$ of order m . As commented in Section 3, U_h^m is spanned by the group of basis functions $\{\lambda_j\}_{j=1}^{n_e}$. Hence, $A_{m,\theta}$ can be expressed as $A_{m,\theta} = (a_{h,\theta}(\lambda_i, \lambda_j))_{n_e \times n_e}$. We define $M_m := (\lambda_i, \lambda_j)_{n_e \times n_e}$ as the mass matrix. For any $\mathbf{v} = \{v_j\}_{j=1}^{n_e} \in \mathbb{R}^{n_e}$, we can associate \mathbf{v} with a finite element function $v_h \in U_h^m$ such that $v_h = \sum_{j=1}^{n_e} v_j \lambda_j$, i.e. \mathbf{v} is the vector of coefficients in (10) for v_h . Conversely, any $v_h \in U_h^m$ has the decomposition $v_h = \sum_{j=1}^{n_e} v_h(\mathbf{x}_{K_j}) \lambda_j$, and we define $\mathbf{v} := \{v_h(\mathbf{x}_{K_j})\}_{j=1}^{n_e} \in \mathbb{R}^{n_e}$ as the corresponding vector for v_h . We have that

$$a_{h,\theta}(v_h, v_h) = \mathbf{v}^T A_{m,\theta} \mathbf{v}, \quad (v_h, v_h)_{L^2(\Omega)} = \mathbf{v}^T M_m \mathbf{v}, \quad \forall v_h \in U_h^m.$$

Let us bound the term $(\mathbf{v}^T M_m \mathbf{v}) / (\mathbf{v}^T \mathbf{v})$, which is established on the constraint in (5). From (5) and the inverse estimate (2), we find that

$$(26) \quad \mathbf{v}^T \mathbf{v} = \sum_{K \in \mathcal{T}_h} (v_h(\mathbf{x}_K))^2 \leq \sum_{K \in \mathcal{T}_h} \|v_h\|_{L^\infty(K)}^2 \leq Ch^{-d} \sum_{K \in \mathcal{T}_h} \|v_h\|_{L^2(K)}^2 = Ch^{-d} \mathbf{v}^T M_m \mathbf{v}, \quad \forall \mathbf{v} \in \mathbb{R}^{n_e}.$$

Again by the constraint in (5), we deduce that

$$(27) \quad \mathbf{v}^T M_m \mathbf{v} \leq Ch^d \sum_{K \in \mathcal{T}_h} \|v_h\|_{L^\infty(K)}^2 \leq Ch^d \Lambda_m^2 \sum_{K \in \mathcal{T}_h} \max_{\mathbf{x} \in I(K)} (v_h(\mathbf{x}))^2 \leq Ch^d \bar{\Lambda}_m^2 \mathbf{v}^T \mathbf{v}, \quad \forall \mathbf{v} \in \mathbb{R}^{n_e}.$$

Combining (26) and (27) yields that

$$(28) \quad Ch^d \leq \frac{\mathbf{v}^T M_m \mathbf{v}}{\mathbf{v}^T \mathbf{v}} \leq C \bar{\Lambda}_m^2 h^d, \quad \forall \mathbf{v} \neq \mathbf{0} \in \mathbb{R}^{n_e}.$$

For the symmetric case $\theta = -1$, we have that

$$(29) \quad \frac{\mathbf{v}^T A_{m,\theta} \mathbf{v}}{\mathbf{v}^T \mathbf{v}} = \frac{a_{h,\theta}(v_h, v_h)}{(v_h, v_h)_{L^2(\Omega)}} \frac{\mathbf{v}^T M_m \mathbf{v}}{\mathbf{v}^T \mathbf{v}}, \quad \forall \mathbf{v} \neq \mathbf{0} \in \mathbb{R}^{n_e}$$

Collecting the boundedness (21), the coercivity (22) and the estimate (20) immediately brings us that

$$\|v_h\|_{L^2(\Omega)}^2 \leq C a_{h,\theta}(v_h, v_h) \leq Ch^{-2} \|v_h\|_{L^2(\Omega)}^2, \quad \forall v_h \in U_h^m.$$

From (28), there holds

$$(30) \quad Ch^d \leq \frac{\mathbf{v}^T A_{m,\theta} \mathbf{v}}{\mathbf{v}^T \mathbf{v}} \leq Ch^{d-2} \bar{\Lambda}_m^2, \quad \forall \mathbf{v} \neq \mathbf{0} \in \mathbb{R}^{n_e},$$

which indicates that $\kappa(A_{m,\theta}) \leq C \bar{\Lambda}_m^2 h^{-2}$ for the symmetric case.

Next, we turn to the nonsymmetric case, i.e. $\theta = 1$. We split the bilinear form $a_{h,\theta}(\cdot, \cdot)$ into a symmetric part and an antisymmetric part. We define the following bilinear forms

$$a_{h,\theta}^S(v_h, w_h) := \sum_{K \in \mathcal{T}_h} \int_K A \nabla v_h \cdot \nabla w_h \, d\mathbf{x} + \sum_{e \in \mathcal{E}_h} \int_e \mu h_e^{-1} [v_h] \cdot [w_h] \, d\mathbf{s}, \quad \forall v_h, w_h \in U_h^m$$

and

$$a_{h,\theta}^N(v_h, w_h) := \sum_{e \in \mathcal{E}_h} \int_e \{A \nabla v_h\} \cdot [w_h] \, d\mathbf{s} - \sum_{e \in \mathcal{E}_h} \int_e \{A \nabla w_h\} \cdot [v_h] \, d\mathbf{s}, \quad \forall v_h, w_h \in U_h^m.$$

Clearly, there holds $a_{h,\theta}(v_h, w_h) = a_{h,\theta}^S(v_h, w_h) - a_{h,\theta}^N(v_h, w_h)$ for $\forall v_h, w_h \in U_h^m$. We denote by $A_{m,\theta}^S$ and by $A_{m,\theta}^N$ the symmetric/antisymmetric linear systems to $a_{h,\theta}^S(\cdot, \cdot)$ and $a_{h,\theta}^N(\cdot, \cdot)$, respectively. We have that $A_{m,\theta} = A_{m,\theta}^S - A_{m,\theta}^N$. From Lemma 5, it can be easily seen that

$$(31) \quad \begin{aligned} |a_{h,\theta}^S(v_h, w_h)| + |a_{h,\theta}^N(v_h, w_h)| &\leq C \|v_h\|_{\text{DG}} \|w_h\|_{\text{DG}}, \quad \forall v_h, w_h \in U_h^m, \\ a_{h,\theta}^S(v_h, v_h) &\geq C \|v_h\|_{\text{DG}}^2, \quad \forall v_h \in U_h^m. \end{aligned}$$

Similar to $A_{m,\theta}$ with $\theta = -1$, the symmetric part $A_{m,\theta}^S$ also satisfies the estimate (30), which gives the estimate $\kappa(A_{m,\theta}^S) \leq C \bar{\Lambda}_m^2 h^{-2}$.

For any $\mathbf{v}, \mathbf{w} \in \mathbb{R}^{n_e}$ with $\|\mathbf{v}\|_{l^2} = \|\mathbf{w}\|_{l^2} = 1$, we have that

$$\begin{aligned} \mathbf{v}^T A_{h,\theta}^N \mathbf{w} &= a_{h,\theta}^N(v_h, w_h) \leq C \|v_h\|_{\text{DG}} \|w_h\|_{\text{DG}} \leq Ch^{-2} \|v_h\|_{L^2(\Omega)} \|w_h\|_{L^2(\Omega)} \\ &\leq Ch^{-2} (\mathbf{v}^T M_m \mathbf{v})^{1/2} (\mathbf{w}^T M_m \mathbf{w})^{1/2} \leq C \bar{\Lambda}_m^2 h^{d-2}. \end{aligned}$$

Since $A_{m,\theta}^N$ is antisymmetric, all eigenvalues are purely imaginary. Then, the spectral radius of $A_{m,\theta}^N$ satisfies that $\rho(A_{m,\theta}^N) \leq C \bar{\Lambda}_m^2 h^{d-2}$. From $A_{m,\theta} = A_{m,\theta}^S - A_{m,\theta}^N$, we conclude that $\kappa(A_{m,\theta}) \leq C \bar{\Lambda}_m^2 h^{-2}$.

Consequently, we have the following estimate to the upper bound of the condition number.

Theorem 2. *Let the penalty parameter μ be defined as in Lemma 5, there exists a constant C such that*

$$(32) \quad \kappa(A_{m,\theta}) \leq C \bar{\Lambda}_m^2 h^{-2}, \quad \theta = \pm 1.$$

By (32), the condition number is the same as in the standard finite element method, i.e. $O(h^{-2})$. As h tends to 0, the matrix $A_{m,\theta}$ becomes ill-conditioned. Hence, an effective preconditioner is desired in finite element methods especially for the high-order accuracy. In the reconstructed approximation, one of attractive features is that the matrix $A_{m,\theta}$ always has the size $n_e \times n_e$, independent of the degree m . Consider the matrix that corresponds to the bilinear form $a_{h,\theta}(\cdot, \cdot)$ over the piecewise constant spaces $U_h^0 \times U_h^0$, and clearly, this matrix still has the size $n_e \times n_e$. We will show that this matrix can be used as an effective preconditioner. We define the bilinear form $a_h^0(\cdot, \cdot)$ as

$$(33) \quad a_h^0(v_h, w_h) = \sum_{e \in \mathcal{E}_h} \int_e h_e^{-1} [v_h] \cdot [w_h] \, d\mathbf{s}, \quad \forall v_h, w_h \in U_h^0,$$

which corresponds to the bilinear form $a_{h,\theta}(\cdot, \cdot)$ over the spaces $U_h^0 \times U_h^0$ in the sense that $a_{h,\theta}(v_h, w_h) = \mu a_h^0(v_h, w_h)$ for $\forall v_h, w_h \in U_h^0$ and $\theta = \pm 1$. Because $a_h^0(v_h, v_h) = \|v_h\|_{\text{DG}}^2$ for $\forall v_h \in U_h^0$, $a_h^0(\cdot, \cdot)$ is bounded and coercive under the energy norm $\|\cdot\|_{\text{DG}}$. Let A_0 be the matrix of $a_h^0(\cdot, \cdot)$. Clearly, A_0 is a symmetric positive definite matrix, and we will show that $\kappa(A_0^{-1}A_{m,\theta}) \leq C\bar{\Lambda}_m^2$ for both $\theta = \pm 1$.

For any piecewise constant function $v_h \in U_h^0$, we know that $\mathcal{R}^m v_h \in U_h^m$ is a piecewise m -th degree polynomial function after the reconstruction. The following equivalence between $\|v_h\|_{\text{DG}}$ and $\|\mathcal{R}^m v_h\|_{\text{DG}}$ is crucial in the analysis.

Lemma 7. *There exist constants C such that*

$$(34) \quad \|v_h\|_{\text{DG}} \leq C\|\mathcal{R}^m v_h\|_{\text{DG}} \leq C\bar{\Lambda}_m\|v_h\|_{\text{DG}}, \quad \forall v_h \in U_h^0.$$

Proof. We first prove the lower bound in (34), i.e.

$$\sum_{e \in \mathcal{E}_h} h_e^{-1} \|[v_h]\|_{L^2(e)}^2 \leq C \left(\sum_{K \in \mathcal{T}_h} \|\nabla \mathcal{R}^m v_h\|_{L^2(K)}^2 + \sum_{e \in \mathcal{E}_h} h_e^{-1} \|\mathcal{R}^m v_h\|_{L^2(e)}^2 \right), \quad \forall v_h \in U_h^0.$$

For any interior face $e \in \mathcal{E}_h^I$, we let e be shared by two elements K_0, K_1 , i.e. $e = \partial K_0 \cap \partial K_1$. From the constraint in (5), we know that $(\mathcal{R}^m v_h)(\mathbf{x}_{K_0}) = (\mathcal{R}_{K_0}^m v_h)(\mathbf{x}_{K_0}) = v_h(\mathbf{x}_{K_0})$ and $(\mathcal{R}^m v_h)(\mathbf{x}_{K_1}) = (\mathcal{R}_{K_1}^m v_h)(\mathbf{x}_{K_1}) = v_h(\mathbf{x}_{K_1})$. Let \mathbf{x}_e be any point on e , together with the inverse estimate (2), we deduce that

$$\begin{aligned} h_e^{-1} \|[v_h]\|_{L^2(e)}^2 &\leq Ch_e^{d-2} (v_h(\mathbf{x}_{K_0}) - v_h(\mathbf{x}_{K_1}))^2 = Ch_e^{d-2} ((\mathcal{R}_{K_0}^m v_h)(\mathbf{x}_{K_0}) - (\mathcal{R}_{K_1}^m v_h)(\mathbf{x}_{K_1}))^2 \\ &\leq Ch_e^{d-2} ((\mathcal{R}_{K_0}^m v_h)(\mathbf{x}_{K_0}) - (\mathcal{R}_{K_0}^m v_h)(\mathbf{x}_e))^2 \\ &\quad + ((\mathcal{R}_{K_1}^m v_h)(\mathbf{x}_{K_1}) - (\mathcal{R}_{K_1}^m v_h)(\mathbf{x}_e))^2 + ((\mathcal{R}_{K_0}^m v_h)(\mathbf{x}_e) - (\mathcal{R}_{K_1}^m v_h)(\mathbf{x}_e))^2 \\ &\leq Ch_e^{d-2} (h_{K_0}^2 \|\nabla \mathcal{R}_{K_0}^m v_h\|_{L^\infty(K_0)}^2 + h_{K_1}^2 \|\nabla \mathcal{R}_{K_1}^m v_h\|_{L^\infty(K_1)}^2 + \|\mathcal{R}^m v_h\|_{L^\infty(e)}^2) \\ &\leq C(\|\nabla \mathcal{R}_{K_0}^m v_h\|_{L^2(K_0)}^2 + \|\nabla \mathcal{R}_{K_1}^m v_h\|_{L^2(K_1)}^2) + h_e^{-1} \|\mathcal{R}^m v_h\|_{L^2(e)}^2. \end{aligned}$$

For any boundary face $e \in \mathcal{E}_h^B$, we let e be a face of an element K_e . Similarly, we have that $(\mathcal{R}^m v_h)(\mathbf{x}_{K_e}) = (\mathcal{R}_{K_e}^m v_h)(\mathbf{x}_{K_e}) = v_h(\mathbf{x}_{K_e})$. Let \mathbf{x}_e be any point on e , we have that

$$\begin{aligned} h_e^{-1} \|v_h\|_{L^2(e)}^2 &= h_e^{d-2} (v_h(\mathbf{x}_{K_e}))^2 = h_e^{d-2} ((\mathcal{R}_{K_e}^m v_h)(\mathbf{x}_{K_e}))^2 \\ &\leq Ch_e^{d-2} ((\mathcal{R}_{K_e}^m v_h)(\mathbf{x}_{K_e}) - (\mathcal{R}_{K_e}^m v_h)(\mathbf{x}_e))^2 + ((\mathcal{R}_{K_e}^m v_h)(\mathbf{x}_e))^2 \\ &\leq C(\|\nabla \mathcal{R}_{K_e}^m v_h\|_{L^2(K_e)}^2) + h_e^{-1} \|\mathcal{R}_{K_e}^m v_h\|_{L^2(e)}^2. \end{aligned}$$

Summation over all faces yields that $\|v_h\|_{\text{DG}} \leq C\|\mathcal{R}^m v_h\|_{\text{DG}}$. The lower bound of (34) is reached.

Then, we focus on the upper bound, i.e.

$$\sum_{K \in \mathcal{T}_h} \|\nabla \mathcal{R}^m v_h\|_{L^2(K)}^2 + \sum_{e \in \mathcal{E}_h} h_e^{-1} \|\mathcal{R}^m v_h\|_{L^2(e)}^2 \leq C\bar{\Lambda}_m^2 \sum_{e \in \mathcal{E}_h} h_e^{-1} \|[v_h]\|_{L^2(e)}^2, \quad \forall v_h \in U_h^0.$$

For $v_h \in U_h^0$, we let $v_{K,\max} := \max_{\mathbf{x} \in I(K)} v_h(\mathbf{x})$ and $v_{K,\min} := \min_{\mathbf{x} \in I(K)} v_h(\mathbf{x})$ for $\forall K \in \mathcal{T}_h$. We apply the inverse estimate (2) and Lemma 3 to see that for $\forall K \in \mathcal{T}_h$, there holds

$$(35) \quad \begin{aligned} \|\nabla \mathcal{R}^m v_h\|_{L^2(K)}^2 &= \|\nabla \mathcal{R}_K^m v_h\|_{L^2(K)}^2 = \|\nabla (\mathcal{R}_K^m v_h - v_{K,\min})\|_{L^2(K)}^2 \leq Ch_K^{d-2} \|\mathcal{R}_K^m (v_h - v_{K,\min})\|_{L^\infty(K)}^2 \\ &\leq Ch_K^{d-2} \bar{\Lambda}_m^2 \max_{\mathbf{x} \in I(K)} |v_h(\mathbf{x}) - v_{K,\min}|^2 \leq Ch_K^{d-2} \bar{\Lambda}_m^2 (v_{K,\max} - v_{K,\min})^2. \end{aligned}$$

For any interior face $e \in \mathcal{E}_h^I$, we also let e be shared by K_0 and K_1 , and we derive that

$$\begin{aligned} h_e^{-1} \|\mathcal{R}^m v_h\|_{L^2(e)}^2 &= h_e^{-1} \|\mathcal{R}_{K_0}^m v_h - \mathcal{R}_{K_1}^m v_h\|_{L^2(e)}^2 \\ &= h_e^{-1} \|\mathcal{R}_{K_0}^m v_h - (\mathcal{R}_{K_0}^m v_h)(\mathbf{x}_{K_0}) - \mathcal{R}_{K_1}^m v_h + (\mathcal{R}_{K_1}^m v_h)(\mathbf{x}_{K_1}) + (\mathcal{R}_{K_0}^m v_h)(\mathbf{x}_{K_0}) - (\mathcal{R}_{K_1}^m v_h)(\mathbf{x}_{K_1})\|_{L^2(e)}^2 \\ &\leq Ch_e^{-1} (h_{K_0}^{d+1} \|\nabla \mathcal{R}_{K_0}^m v_h\|_{L^\infty(K_0)}^2 + h_{K_1}^{d+1} \|\nabla \mathcal{R}_{K_1}^m v_h\|_{L^\infty(K_1)}^2) + Ch_e^{d-2} (v_h(\mathbf{x}_{K_0}) - v_h(\mathbf{x}_{K_1}))^2 \\ &\leq C(\|\nabla \mathcal{R}_{K_0}^m v_h\|_{L^2(K_0)}^2 + \|\nabla \mathcal{R}_{K_1}^m v_h\|_{L^2(K_1)}^2) + h_e^{-1} \|[v_h]\|_{L^2(e)}^2. \end{aligned}$$

For any boundary face $e \in \mathcal{E}_h^B$, we let e be a face of an element K_e , and there holds

$$h_e^{-1} \|\mathcal{R}^m v_h\|_{L^2(e)}^2 = h_e^{-1} \|\mathcal{R}_{K_e}^m v_h\|_{L^2(e)}^2 \leq C(\|\nabla \mathcal{R}_{K_e}^m v_h\|_{L^2(K_e)}^2 + h_e^{-1} \|[v_h]\|_{L^2(e)}^2).$$

Collecting above two estimates brings us that

$$(36) \quad \|\mathcal{R}^m v_h\|_{\text{DG}}^2 \leq C\bar{\Lambda}_m^2 \sum_{K \in \mathcal{T}_h} h_K^{d-2} (v_{K,\max} - v_{K,\min})^2 + C\|v_h\|_{\text{DG}}^2.$$

For $\forall K \in \mathcal{T}_h$, we let $\mathcal{E}_{S(K)} := \bigcup_{K' \in S(K)} \mathcal{E}_{K'}$, where $\mathcal{E}_{K'} := \{e \in \mathcal{E}_h \mid e \subset \partial K'\}$, be the set of all faces corresponding to all elements in $S(K)$. We then show that for $\forall K \in \mathcal{T}_h$, there holds

$$(37) \quad (v_{K,\max} - v_{K,\min})^2 \leq C \sum_{e \in \mathcal{E}_{S(K)}} h_e^{1-d} \| [v_h] \|_{L^2(e)}^2.$$

Let $K', K'' \in S(K)$ such that $v_{K,\max} = v_h|_{K'}$ and $v_{K,\min} = v_h|_{K''}$. Clearly, there exists a sequence $\tilde{K}_0, \tilde{K}_1, \dots, \tilde{K}_M$ such that $\tilde{K}_0 = K'$, $\tilde{K}_M = K''$, $\tilde{K}_j \in S(K)$ ($0 \leq j \leq M$), and \tilde{K}_j is adjacent to \tilde{K}_{j+1} , and we let $\tilde{e}_j = \partial \tilde{K}_j \cap \partial \tilde{K}_{j+1}$. We have that

$$(v_{K,\max} - v_{K,\min})^2 \leq C \sum_{j=0}^{M-1} (v_h|_{\tilde{K}_j} - v_h|_{\tilde{K}_{j+1}})^2 \leq C \sum_{j=0}^{M-1} h_{\tilde{e}_j}^{1-d} \| [v_h] \|_{L^2(\tilde{e}_j)}^2 \leq C \sum_{e \in \mathcal{E}_{S(K)}} h_e^{1-d} \| [v_h] \|_{L^2(e)}^2.$$

Combining (36) and (37) leads to the upper bound in (34). This completes the proof. \square

The condition number of the preconditioned system $A_0^{-1}A_{m,\theta}$ will be established on Lemma 7. We begin the analysis from the symmetric case, i.e. $\theta = -1$. In the estimation of the condition number to the matrix $A_{m,\theta}$, we stated that any vector $\mathbf{v} \in \mathbb{R}^{n_e}$ corresponds to a finite element function $v_h \in U_h^m$. For the analysis to the preconditioned system, we let any $\mathbf{v} = \{v_j\}_{j=1}^{n_e} \in \mathbb{R}^{n_e}$ correspond to a piecewise constant function $v_h \in U_h^0$ such that $v_h(\mathbf{x}_K) = v_j$, where K is the element indexed by j . Now, we have that

$$\mathbf{v}^T A_0 \mathbf{w} = a_h^0(v_h, w_h), \quad \mathbf{v}^T A_{m,\theta} \mathbf{w} = a_{h,\theta}(\mathcal{R}^m v_h, \mathcal{R}^m w_h), \quad \forall \mathbf{v}, \mathbf{w} \in \mathbb{R}^{n_e}.$$

By Lemma 7 and the boundedness and the coercivity of $a_{h,\theta}(\cdot, \cdot)$, we find that

$$(38) \quad C_0 \bar{\Lambda}_m^{-2} \mathbf{v}^T A_{m,\theta} \mathbf{v} \leq \mathbf{v}^T A_0 \mathbf{v} \leq C_1 \mathbf{v}^T A_{m,\theta} \mathbf{v}, \quad \forall \mathbf{v} \in \mathbb{R}^{n_e}.$$

From [41, Lemma 2.1], the above estimate yields the desired estimate $\kappa(A_0^{-1}A_{m,\theta}) \leq C\bar{\Lambda}_m^2$ for the symmetric case $\theta = -1$.

Next, we consider the preconditioned system for the nonsymmetric case $\theta = 1$. In this case, we have that

$$(39) \quad \mathbf{v}^T A_{h,\theta}^S \mathbf{w} = a_{h,\theta}^S(\mathcal{R}^m v_h, \mathcal{R}^m w_h), \quad \mathbf{v}^T A_{h,\theta}^N \mathbf{w} = a_{h,\theta}^N(\mathcal{R}^m v_h, \mathcal{R}^m w_h), \quad \forall \mathbf{v}, \mathbf{w} \in \mathbb{R}^{n_e}.$$

The matrix $A_0^{-1}A_{m,\theta}$ can be split as $A_0^{-1}A_{m,\theta} = A_0^{-1}A_{m,\theta}^S - A_0^{-1}A_{m,\theta}^N$. From (39), the estimate (38) also holds for the symmetric part $A_{m,\theta}^S$, which gives that $\kappa(A_0^{-1}A_{m,\theta}^S) \leq C\bar{\Lambda}_m^2$. For the antisymmetric part, we deduce that

$$(40) \quad \begin{aligned} \mathbf{v}^T A_{h,\theta}^N \mathbf{w} &= a_{h,\theta}^N(\mathcal{R}^m v_h, \mathcal{R}^m w_h) \leq C \|\mathcal{R}^m v_h\|_{\text{DG}} \|\mathcal{R}^m w_h\|_{\text{DG}} \leq C\bar{\Lambda}_m^2 \|v_h\|_{\text{DG}} \|w_h\|_{\text{DG}} \\ &\leq C\bar{\Lambda}_m^2 \sqrt{\mathbf{v}^T A_0 \mathbf{v}} \sqrt{\mathbf{w}^T A_0 \mathbf{w}}, \end{aligned}$$

which implies that the spectral radius of the system $A_0^{-1}A_{h,\theta}^N$ satisfies that $\rho(A_0^{-1}A_{h,\theta}^N) \leq C\bar{\Lambda}_m^2$.

Ultimately, we summarize the estimation of the condition number for the preconditioned system in the following theorem.

Theorem 3. *Let μ be defined as in Lemma 5, there exists a constant C such that*

$$(41) \quad \kappa(A_0^{-1}A_{m,\theta}) \leq C\bar{\Lambda}_m^2, \quad \theta = \pm 1.$$

Remark 3. *The estimate of the condition number is based on the boundedness and the coercivity of the bilinear form $a_{h,\theta}(\cdot, \cdot)$, i.e.*

$$\widehat{C} \|v_h\|_{\text{DG}}^2 \leq a_{h,\theta}(v_h, v_h) \leq \widetilde{C} \|v_h\|_{\text{DG}}^2, \quad \forall v_h \in U_h^m.$$

For the symmetric scheme, by (29) and (38) we obtain that the constants in (32) and (41) depend on $\widetilde{C}/\widehat{C}$, i.e. $\kappa(A_{m,\theta}) \leq C_0(\widetilde{C}/\widehat{C})\bar{\Lambda}_m^2 h^{-2}$ and $\kappa(A_0^{-1}A_{m,\theta}) \leq C_1(\widetilde{C}/\widehat{C})\bar{\Lambda}_m^2$, where C_0 and C_1 are independent of μ and A . We refer to [21] for the detailed analysis of the relationship between \widehat{C} , \widetilde{C} and the penalty parameter μ and the coefficient A .

By Theorem 3, the resulting linear system $A_{m,\theta}\mathbf{x} = \mathbf{b}$ can be solved by using an iterative approach from the Krylov-subspace family with the preconditioner A_0^{-1} . In numerical tests, the preconditioned CG/GMRES methods are applied to the symmetric/nonsymmetric linear systems, respectively. For the nonsymmetric system, we present more details about the convergence analysis to the GMRES solver. We

define an inner product $(\mathbf{v}, \mathbf{w})_{A_0} := \mathbf{v}^T A_0 \mathbf{w}$ for $\forall \mathbf{v}, \mathbf{w} \in \mathbb{R}^{n_e}$ and its induced norm by $\|\cdot\|_{A_0}$. By [42, Theorem 1], the convergence estimate of the preconditioned GMRES method follows from the estimates

$$(42) \quad \|A_0^{-1} A_{m,1} \mathbf{v}\|_{A_0} \leq C_0 \bar{\Lambda}_m^2 \|\mathbf{v}\|_{A_0}, \quad \forall \mathbf{v} \in \mathbb{R}^{n_e},$$

and

$$(43) \quad (A_0^{-1} A_{m,1} \mathbf{v}, \mathbf{v})_{A_0} \geq C_1 (\mathbf{v}, \mathbf{v})_{A_0}, \quad \forall \mathbf{v} \in \mathbb{R}^{n_e}.$$

From (39) and (38), we derive that

$$(A_0^{-1} A_{m,1} \mathbf{v}, \mathbf{v})_{A_0} = \mathbf{v}^T A_{m,1} \mathbf{v} = \mathbf{v}^T A_{m,1}^S \mathbf{v} \geq C \mathbf{v}^T A_0 \mathbf{v} = C (\mathbf{v}, \mathbf{v})_{A_0}, \quad \forall \mathbf{v} \in \mathbb{R}^{n_e},$$

which gives the second estimate (43). By letting $\mathbf{x} = A_0^{1/2} \mathbf{v}$ and $\mathbf{y} = A_0^{1/2} \mathbf{w}$ in (40), we find that

$$\mathbf{x}^T A_0^{-1/2} A_{m,1}^N A_0^{-1/2} \mathbf{y} \leq C \bar{\Lambda}_m^2 \sqrt{\mathbf{x}^T \mathbf{x}} \sqrt{\mathbf{y}^T \mathbf{y}}, \quad \forall \mathbf{x}, \mathbf{y} \in \mathbb{R}^{n_e},$$

which leads to $\sigma_{\max}(A_0^{-1/2} A_{m,1}^N A_0^{-1/2}) \leq C \bar{\Lambda}_m^2$. From the triangle inequality, we have that

$$\|A_0^{-1} A_{m,1} \mathbf{v}\|_{A_0} \leq \|A_0^{-1} A_{m,1}^S \mathbf{v}\|_{A_0} + \|A_0^{-1} A_{m,1}^N \mathbf{v}\|_{A_0}, \quad \forall \mathbf{v} \in \mathbb{R}^{n_e}.$$

By (38) and [41, Lemma 2.1], there holds

$$\|A_0^{-1} A_{m,1}^S \mathbf{v}\|_{A_0}^2 = \mathbf{v}^T A_{m,1}^S A_0^{-1} A_{m,1}^S \mathbf{v} \leq C \bar{\Lambda}_m^4 \mathbf{v}^T A_0 \mathbf{v} = C \bar{\Lambda}_m^4 \|\mathbf{v}\|_{A_0}^2, \quad \forall \mathbf{v} \in \mathbb{R}^{n_e}.$$

For the second term, we derive that

$$\begin{aligned} \|A_0^{-1} A_{m,1}^N \mathbf{v}\|_{A_0}^2 &= \mathbf{v}^T (A_{m,1}^N)^T A_0^{-1} A_{m,1}^N \mathbf{v} \\ &= \mathbf{w}^T (A_0^{-1/2} A_{m,1}^N A_0^{-1/2})^T A_0^{-1/2} A_{m,1}^N A_0^{-1/2} \mathbf{w} \quad (\text{let } \mathbf{w} = A_0^{1/2} \mathbf{v}) \\ &\leq (\sigma_{\max}(A_0^{-1/2} A_{m,1}^N A_0^{-1/2}))^2 \mathbf{w}^T \mathbf{w} \leq C \bar{\Lambda}_m^4 \mathbf{v}^T A_0 \mathbf{v} = C \bar{\Lambda}_m^4 \|\mathbf{v}\|_{A_0}^2, \quad \forall \mathbf{v} \in \mathbb{R}^{n_e}. \end{aligned}$$

The estimate (42) is reached. From (42) and (43), the preconditioned GMRES method for solving the system $A_{m,1} \mathbf{x} = \mathbf{b}$ has the following convergence rate [42, Theorem 2],

$$\|\mathbf{r}_k\|_{A_0} \leq (1 - (C_1/(C_0 \bar{\Lambda}_m^2))^2)^{k/2} \|\mathbf{r}_0\|_{A_0}.$$

where $\mathbf{r}_k = \mathbf{b} - A_{m,1} \mathbf{x}_k$ is the residual at the iteration step k .

In the Krylov iteration step, we are required to compute the matrix-vector product $A_0^{-1} \mathbf{y}$. Hence, a fast and accurate method to solve the linear system of the form $A_0 \mathbf{z} = \mathbf{y}$ is desired in our scheme. On the triangular meshes, we outline a \mathcal{V} -cycle multigrid method for this system. Let $\mathcal{T}_1, \mathcal{T}_2, \dots, \mathcal{T}_r$ be a series of successively refined meshes, i.e. \mathcal{T}_{l+1} is created by subdividing all of triangular (tetrahedral) elements in \mathcal{T}_l . Let U_l^0 be the piecewise constant space on the partition \mathcal{T}_l , and we have that

$$U_1^0 \subset U_2^0 \subset U_3^0 \dots \subset U_r^0.$$

We let $I_k^{k+1} : U_k^0 \rightarrow U_{k+1}^0$ be the canonical prolongation operator, i.e. $I_k^{k+1} v_h = v_h (\forall v_h \in U_k^0)$, and we let $I_{k+1}^k : U_{k+1}^0 \rightarrow U_k^0$ be the transpose of I_k^{k+1} . Let A_k^0 be the matrix for the bilinear form $a_h^0(\cdot, \cdot)$ over the spaces $U_k^0 \times U_k^0$. Then, the standard recursive structure of the multigrid algorithm is depicted in Algorithm 1. Consequently, the preconditioner in preconditioned CG/GMRES methods to the linear system $A_{m,\theta} \mathbf{x} = \mathbf{b}$ can be chosen as Algorithm 1. We also apply the algebraic multigrid method (BoomerAMG in the package HYPRE [22]) and the direct LU method to approximate A_0^{-1} to precondition the linear system. The three different preconditioners give a close convergence step for CG/GMRES solvers in numerical results. The theoretical analysis for multigrid methods in approximating A_0^{-1} is considered as a future work for us.

5. NUMERICAL RESULTS

In this section, a series of numerical experiments are conducted to demonstrate the performance of the proposed method and the efficiency of the preconditioning method. The meshes we used in the following examples are shown in Fig. 1. The threshold $\#S$ used in all tests are listed in Tab. 1 and Tab. 2. For the symmetric scheme $\theta = -1$, we take the penalty parameter $\mu = 3m^2 + 5$, and for the nonsymmetric scheme $\theta = 1$, we fix the penalty parameter $\mu = 1$.

5.1. Study on convergence rate. We first demonstrate the convergence behavior to examine the theoretical predictions and show the efficiency of the proposed method.

Algorithm 1: \mathcal{V} -cycle Multigrid Solver, $\text{MGSolver}(\mathbf{x}_k, \mathbf{b}_k, k)$ **Input:** the initial guess \mathbf{x}_k , the right hand side \mathbf{b}_k , the level k ;**Output:** the solution \mathbf{x}_k ;**if** $k = 1$ **then** $\mathbf{x}_1 = (A_1^0)^{-1}\mathbf{b}_1$, \mathbf{x}_1 is the solution obtained from a direct method; return \mathbf{x}_1 ;**if** $k > 1$ **then** pre-smoothing step: Gauss-Seidel sweep on $A_k^0\mathbf{x}_k = \mathbf{b}_k$; error correction step: let $\mathbf{y} = I_k^{k-1}(\mathbf{b}_k - A_k^0\mathbf{x}_k)$, and let $\mathbf{z}_0 = \mathbf{0}$, and let

$$\mathbf{z}_1 = \text{MGSolver}(\mathbf{z}_0, \mathbf{y}, k-1);$$

 set $\mathbf{x}_k = \mathbf{x}_k + I_{k-1}^k\mathbf{z}_1$. post-smoothing step: Gauss-Seidel sweep on $A_k^0\mathbf{x}_k = \mathbf{b}_k$; return \mathbf{x}_k ;

| m | | 1 | 2 | 3 | 4 |
|----------------------|---------------------|---|----|----|----|
| $\#S$ | the triangular mesh | 5 | 9 | 15 | 21 |
| | the polygonal mesh | 6 | 10 | 16 | 23 |
| $\dim(\mathbb{P}_m)$ | | 3 | 6 | 10 | 15 |

TABLE 1. The threshold $\#S$ in two dimensions.

| m | | 1 | 2 | 3 |
|-------|----------------------|---|----|----|
| $\#S$ | the tetrahedral mesh | 9 | 19 | 38 |
| | $\dim(\mathbb{P}_m)$ | 4 | 10 | 20 |

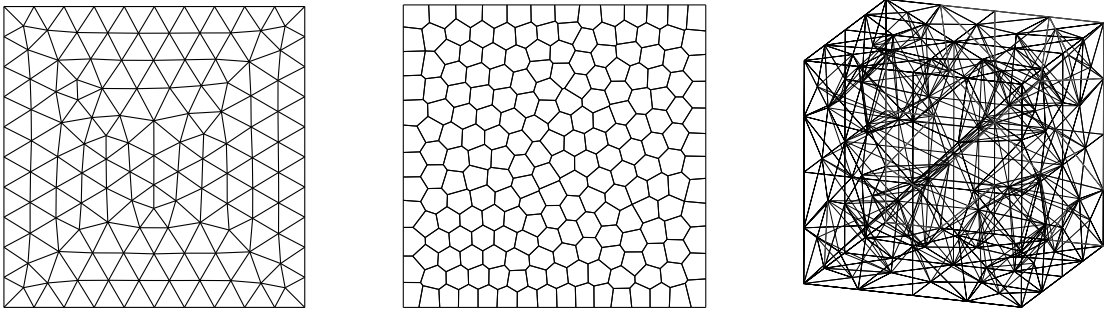
TABLE 2. The threshold $\#S$ in three dimensions.

FIGURE 1. The triangular mesh (left), polygonal mesh (middle) and tetrahedral mesh (right).

Example 1. In the first example, we consider an elliptic problem in the squared domain $\Omega = (-1, 1)^2$. The coefficient matrix A is taken as the identical matrix I , and the exact solution $u(x, y)$ is given by

$$u(x, y) = \sin(2\pi(x + y)) \sin(2\pi y) + x^2 y.$$

We solve this problem with the reconstructed space U_h^m , and the numerical results are displayed in Tab. 3. Clearly, the numerical errors under both the energy norm and the L^2 norm approach zero at the optimal convergence rates, which confirm the theoretical results.

According to [25], the number of degrees of freedom to the specific discrete system can serve as a proper indicator for the scheme's efficiency. This indicator mainly reveals the efficiency of the finite element approximation to Sobolev spaces. For the proposed scheme, the number of degrees of freedom is always the number of elements in the partition. Let $V_h^m := \{v_h \in L^2(\Omega) \mid v_h|_K \in \mathbb{P}_m(K), \forall K \in \mathcal{T}_h\}$, which is usually the approximation space in the standard DG method. We also solve this problem by the space V_h^m . The L^2 errors for both methods against the number of degrees of freedom are plotted in

Fig. 2. It can be observed that fewer degrees of freedom are needed by the reconstructed space to achieve a comparable L^2 error. Tab. 4 lists the ratio of the number of degrees of freedom by two methods when the same L^2 errors are achieved. The saving of degrees of freedom is more remarkable for U_h^m when using the high-order approximation.

| m | h | 1/10 | 1/20 | 1/40 | 1/80 | 1/160 | order |
|-----|-----------------------------|---------|---------|---------|---------|---------|-------|
| 1 | $\ u - u_h\ _{\text{DG}}$ | 3.98e-0 | 1.93e-0 | 9.30e-1 | 4.55e-1 | 2.25e-1 | 1.03 |
| | $\ u - u_h\ _{L^2(\Omega)}$ | 1.53e-1 | 3.50e-2 | 9.44e-3 | 2.42e-3 | 6.09e-4 | 2.00 |
| 2 | $\ u - u_h\ _{\text{DG}}$ | 1.78e-0 | 4.34e-1 | 1.02e-1 | 2.44e-2 | 5.95e-3 | 2.05 |
| | $\ u - u_h\ _{L^2(\Omega)}$ | 4.69e-2 | 5.41e-3 | 5.93e-4 | 6.81e-5 | 8.17e-6 | 3.06 |
| 3 | $\ u - u_h\ _{\text{DG}}$ | 7.36e-1 | 8.70e-2 | 1.03e-2 | 1.18e-3 | 1.38e-4 | 3.09 |
| | $\ u - u_h\ _{L^2(\Omega)}$ | 1.43e-2 | 7.04e-4 | 3.96e-5 | 2.40e-6 | 1.49e-7 | 4.01 |
| 4 | $\ u - u_h\ _{\text{DG}}$ | 3.34e-1 | 2.02e-2 | 1.32e-3 | 8.03e-5 | 4.80e-6 | 4.02 |
| | $\ u - u_h\ _{L^2(\Omega)}$ | 8.65e-3 | 2.38e-4 | 6.85e-6 | 1.96e-7 | 5.75e-9 | 5.08 |

TABLE 3. The convergence histories for Example 1 with the reconstructed space U_h^m .

Example 2. Next, we consider the elliptic problem in three dimensions defined on the cubic domain $\Omega = (0, 1)^3$. We choose the smooth function

$$u(x, y, z) = \sin(2\pi(x + y + z)),$$

as the exact solution. The coefficient matrix A is taken as the identical matrix I . The convergence histories with the reconstructed space U_h^m are gathered in Tab. 5, which clearly illustrate the predictions in Theorem 1. Then, we solve this problem by the space V_h^m , and the numerical results are reported in Fig. 2 and Tab. 6. One can observe that the reconstructed space U_h^m still has a better performance on the efficiency of the finite element approximation, and the advantage becomes prominent with the increasing of m in three dimensions.

5.2. Study on preconditioned system. In this subsection, we illustrate the efficiency on solving the preconditioned system $A_0^{-1}A_{m,\theta}\mathbf{x} = \mathbf{b}$ in two and three dimensions. For the symmetric and nonsymmetric schemes, the linear systems are solved by the preconditioned CG/GMRES methods, respectively. In Algorithm 1, the number of the presmoothing and postsmoothing steps are fixed as 4. We also use the

| m | 1 | 2 | 3 | 4 |
|---------|-----|-----|-----|-----|
| RDA/DGM | 72% | 53% | 42% | 34% |

TABLE 4. The ratio of the number of degrees of freedom used in U_h^m and V_h^m when achieving a comparable L^2 error in Example 1.

| m | h | 1/4 | 1/8 | 1/16 | 1/32 | order |
|-----|-----------------------------|---------|---------|---------|---------|-------|
| 1 | $\ u - u_h\ _{\text{DG}}$ | 1.23e-0 | 5.95e-1 | 2.89e-1 | 1.43e-1 | 1.03 |
| | $\ u - u_h\ _{L^2(\Omega)}$ | 5.46e-2 | 1.41e-2 | 3.70e-3 | 1.00e-3 | 1.92 |
| 2 | $\ u - u_h\ _{\text{DG}}$ | 3.93e-1 | 9.52e-2 | 2.32e-2 | 5.68e-3 | 2.03 |
| | $\ u - u_h\ _{L^2(\Omega)}$ | 1.51e-2 | 1.99e-3 | 2.43e-4 | 3.09e-5 | 2.98 |
| 3 | $\ u - u_h\ _{\text{DG}}$ | 1.81e-1 | 1.74e-2 | 1.93e-2 | 2.30e-4 | 3.20 |
| | $\ u - u_h\ _{L^2(\Omega)}$ | 7.78e-3 | 3.62e-4 | 2.04e-5 | 1.25e-6 | 4.20 |

TABLE 5. The convergence histories for Example 2 with the reconstructed space U_h^m .

| m | 1 | 2 | 3 |
|---------|-----|-----|-----|
| RDA/DGM | 57% | 46% | 34% |

TABLE 6. The ratio of the number of degrees of freedom used in U_h^m and V_h^m when achieving a comparable L^2 error in Example 2.

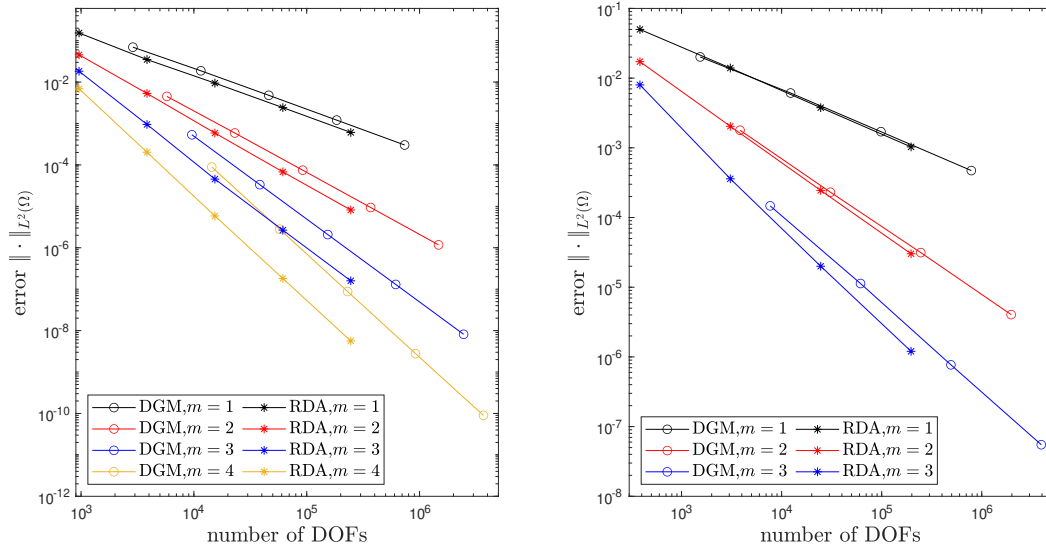


FIGURE 2. The comparison of the L^2 error for the spaces U_h^m and V_h^m in Example 1 (left) / Example 2 (right).

BoomerAMG method and the direct LU method to approximate A_0^{-1} to precondition the linear systems. The iteration stops when the relative error

$$\frac{\|\mathbf{b} - A_{m,\theta} \mathbf{x}_k\|_{l^2}}{\|\mathbf{b}\|_{l^2}}.$$

at the stage k is smaller than the tolerance $\varepsilon = 10^{-8}$.

Example 3. In this example, we examine the condition numbers of the preconditioned system $A_0^{-1}A_{m,\theta}$ for both $\theta = \pm 1$. We assemble the linear system on the triangular meshes with $h = 1/10, 1/20, 1/40$. The condition numbers for different m are gathered in Tab. 7. It can be observed that the condition numbers for both symmetric/nonsymmetric systems are nearly constants as the mesh size h tends to zero. This numerical observation fairly matches the estimate in Theorem 3.

| h | $\kappa(A_0^{-1}A_{m,-1})$ | | | $\kappa(A_0^{-1}A_{m,1})$ | | |
|------|----------------------------|---------|---------|---------------------------|---------|---------|
| | $m = 1$ | $m = 2$ | $m = 3$ | $m = 1$ | $m = 2$ | $m = 3$ |
| 1/10 | 10.73 | 14.81 | 29.28 | 11.48 | 21.61 | 40.90 |
| 1/20 | 11.14 | 17.62 | 27.99 | 12.23 | 23.28 | 39.29 |
| 1/40 | 12.78 | 18.81 | 29.73 | 13.70 | 24.89 | 41.61 |

TABLE 7. The condition numbers of the preconditioned systems in two dimensions.

Example 4. In this example, we solve an elliptic problem on the domain $\Omega = (-1, 1)^2$. We adopt a family of triangular meshes with the mesh size $h = 1/10, 1/20, 1/40, 1/80, 1/160$. The exact solution is chosen to be the same as in Example 1. Tab. 8 lists the convergence steps for CG/GMRES solvers. Besides preconditioning with A_0^{-1} , we try to use the BoomerAMG algorithm to the matrix $A_{m,\theta}$ as the preconditioner, and we also directly apply the standard CG/GMRES methods in solving linear systems. It can be observed that the methods preconditioning with A_0^{-1} have a much faster convergence speed than other methods. For all accuracy $1 \leq m \leq 4$, the convergence steps are numerically detected to be independent of h , which illustrates the results in Theorem 3. Fig. 3 displays the convergence histories of CG/GMRES solvers. The relative errors in iterations of the system $A_0^{-1}A_{m,\theta}$ decrease sharply, compared to the standard CG/GMRES methods. Tab. 9 gives the CPU times in solving the linear system by different methods. It is evident that the CG/GMRES methods, when employing the Algorithm 1 for A_0^{-1} as a preconditioner, is faster than other methods.

As we stated in Remark 2, the element patch will bring more computational cost in assembling the stiffness matrix and increase the width of the banded structure. Tab. 10 lists the CPU times in different

steps for both our symmetric scheme and the standard symmetric DG scheme. It can be observed that for our method, solving local least squares problems per element is very cheap, and as expected, our method requires more CPU time in the step of assembling the stiffness matrix. For our method, the most time-consuming step is assembling the stiffness matrix, and solving the final linear system is much faster than this step. Generally, the step of assembling the stiffness matrix can be easily accelerated by a parallel implementation typically exploiting the multithreading technique. For the DG method solving this example, we also try to apply the preconditioned CG method using BoomerAMG algorithm as the preconditioner. We observe that the step of solving the linear system is more time-consuming compared with assembling the stiffness matrix, which appears to be different from the reconstructed method.

| m | Preconditioner | | $1/h$ | | | | | $1/h$ | | | | |
|-----|----------------|--------------|---------------|------|------|------|------|-----------------|------|------|------|-----|
| | | | 10 | 20 | 40 | 80 | 160 | 10 | 20 | 40 | 80 | 160 |
| | θ | | -1: symmetric | | | | | 1: nonsymmetric | | | | |
| 1 | A_0^{-1} | GMG | 16 | 17 | 18 | 18 | 18 | 23 | 25 | 25 | 26 | 26 |
| | | BoomerAMG | 16 | 17 | 18 | 19 | 20 | 23 | 24 | 26 | 27 | 28 |
| | | DirectSolver | 16 | 17 | 18 | 18 | 18 | 23 | 24 | 25 | 25 | 26 |
| | | BoomerAMG | 15 | 16 | 20 | 26 | 35 | 16 | 20 | 25 | 32 | 47 |
| | | Identity | 109 | 251 | 507 | 1019 | 1994 | 80 | 269 | 827 | 2690 | - |
| 2 | A_0^{-1} | GMG | 20 | 22 | 23 | 23 | 23 | 32 | 32 | 33 | 34 | 35 |
| | | BoomerAMG | 20 | 23 | 24 | 24 | 24 | 33 | 33 | 35 | 35 | 36 |
| | | DirectSolver | 20 | 21 | 23 | 23 | 23 | 32 | 32 | 32 | 33 | 33 |
| | | BoomerAMG | 20 | 25 | 32 | 41 | 63 | 24 | 26 | 31 | 39 | 56 |
| | | Identity | 274 | 548 | 1067 | 2071 | - | 173 | 432 | 994 | 2722 | - |
| 3 | A_0^{-1} | GMG | 44 | 45 | 45 | 46 | 46 | 49 | 51 | 52 | 53 | 54 |
| | | BoomerAMG | 43 | 45 | 45 | 46 | 46 | 48 | 51 | 51 | 51 | 52 |
| | | DirectSolver | 41 | 43 | 44 | 44 | 44 | 48 | 50 | 49 | 49 | 50 |
| | | BoomerAMG | 32 | 35 | 42 | 53 | 70 | 35 | 38 | 41 | 49 | 64 |
| | | Identity | 411 | 806 | 1598 | - | - | 238 | 899 | 2345 | - | - |
| 4 | A_0^{-1} | GMG | 68 | 72 | 73 | 74 | 75 | 60 | 62 | 69 | 74 | 77 |
| | | BoomerAMG | 63 | 68 | 70 | 71 | 71 | 59 | 61 | 66 | 71 | 72 |
| | | DirectSolver | 61 | 66 | 68 | 69 | 68 | 59 | 61 | 66 | 71 | 73 |
| | | BoomerAMG | 60 | 63 | 76 | 86 | 102 | 62 | 67 | 76 | 91 | 105 |
| | | Identity | 588 | 1264 | 2528 | - | - | 290 | 1390 | - | - | - |

TABLE 8. The convergence steps for symmetric and nonsymmetric methods in Example 4.

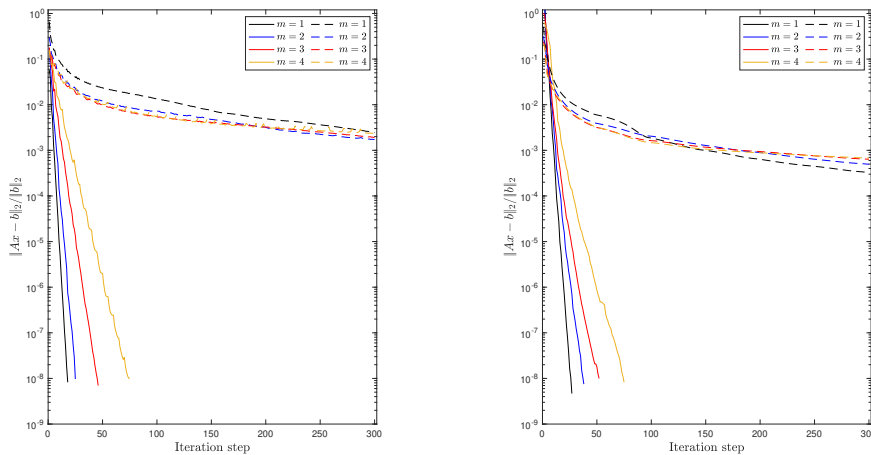


FIGURE 3. The convergence histories of CG (left) /GMRES (right) solvers on the mesh $h = 1/160$ (solid line: CG/GMRES solver with preconditioner A_0^{-1} , dashed line: standard CG/GMRES solver).

| m | $1/h$ | | 10 | 20 | 40 | 80 | 160 | 10 | 20 | 40 | 80 | 160 | |
|----------|------------|--------------|--------------|-------|-------|-------|-------|----------------|-------|-------|-------|-------|--|
| | | | -1:symmetric | | | | | 1:nonsymmetric | | | | | |
| 1 | θ | | | | | | | | | | | | |
| | A_0^{-1} | GMG | 0.002 | 0.010 | 0.036 | 0.160 | 0.744 | 0.002 | 0.011 | 0.044 | 0.200 | 0.982 | |
| | | BoomerAMG | 0.005 | 0.017 | 0.063 | 0.282 | 1.229 | 0.007 | 0.022 | 0.080 | 0.345 | 1.559 | |
| | | DirectSolver | 0.002 | 0.008 | 0.036 | 0.255 | 1.396 | 0.002 | 0.008 | 0.042 | 0.301 | 1.736 | |
| | | BoomerAMG | 0.010 | 0.036 | 0.156 | 0.962 | 5.616 | 0.018 | 0.063 | 0.268 | 1.195 | 7.347 | |
| Identity | 0.015 | 0.096 | 0.753 | 6.025 | 58.90 | 0.009 | 0.065 | 0.614 | 8.416 | - | | | |
| 2 | A_0^{-1} | GMG | 0.004 | 0.013 | 0.057 | 0.256 | 1.112 | 0.004 | 0.018 | 0.075 | 0.352 | 1.497 | |
| | | BoomerAMG | 0.008 | 0.022 | 0.085 | 0.376 | 1.603 | 0.012 | 0.028 | 0.126 | 0.533 | 2.219 | |
| | | DirectSolver | 0.004 | 0.012 | 0.056 | 0.423 | 1.923 | 0.004 | 0.015 | 0.075 | 0.493 | 2.765 | |
| | | BoomerAMG | 0.016 | 0.069 | 0.336 | 1.851 | 12.22 | 0.016 | 0.065 | 0.300 | 1.734 | 10.77 | |
| | Identity | 0.026 | 0.187 | 1.530 | 13.60 | - | 0.013 | 0.142 | 1.341 | 20.23 | - | | |
| 3 | A_0^{-1} | GMG | 0.020 | 0.036 | 0.148 | 0.662 | 2.833 | 0.007 | 0.032 | 0.141 | 0.690 | 2.955 | |
| | | BoomerAMG | 0.013 | 0.049 | 0.187 | 0.820 | 3.512 | 0.013 | 0.059 | 0.203 | 0.854 | 3.650 | |
| | | DirectSolver | 0.009 | 0.032 | 0.150 | 0.862 | 4.479 | 0.006 | 0.027 | 0.132 | 1.093 | 4.625 | |
| | | BoomerAMG | 0.028 | 0.125 | 0.610 | 3.669 | 18.85 | 0.030 | 0.130 | 0.582 | 3.933 | 17.05 | |
| | Identity | 0.058 | 0.427 | 3.529 | - | - | 0.022 | 0.352 | 3.823 | - | - | | |
| 4 | A_0^{-1} | GMG | 0.019 | 0.077 | 0.324 | 1.546 | 6.388 | 0.012 | 0.049 | 0.226 | 1.130 | 5.300 | |
| | | BoomerAMG | 0.024 | 0.089 | 0.370 | 1.567 | 7.229 | 0.018 | 0.066 | 0.304 | 1.649 | 7.544 | |
| | | DirectSolver | 0.016 | 0.068 | 0.327 | 1.856 | 8.563 | 0.016 | 0.043 | 0.237 | 1.460 | 7.847 | |
| | | BoomerAMG | 0.060 | 0.281 | 1.603 | 8.587 | 42.99 | 0.063 | 0.286 | 1.390 | 8.981 | 42.58 | |
| | Identity | 0.120 | 1.027 | 8.490 | - | - | 0.038 | 0.740 | - | - | - | | |

TABLE 9. The CPU times of solving linear systems for symmetric and nonsymmetric methods in Example 4.

| m | h | 1/20 | 1/40 | 1/80 | | |
|-----|-----|--|--|-------|-------|-------|
| 1 | RDA | solve least squares problems | 0.015 | 0.061 | 0.251 | |
| | | assemble the stiffness matrix | 0.155 | 0.636 | 2.626 | |
| | | solve the linear system by CG + A_0^{-1} | 0.010 | 0.036 | 0.160 | |
| | DGM | assemble the stiffness matrix | 0.052 | 0.206 | 0.826 | |
| | | solve the linear system by CG + AMG | 0.076 | 0.313 | 1.662 | |
| | | solve least squares problems | 0.047 | 0.181 | 0.739 | |
| 2 | RDA | assemble the stiffness matrix | 0.578 | 2.332 | 9.378 | |
| | | solve the linear system by CG + A_0^{-1} | 0.013 | 0.057 | 0.256 | |
| | | assemble the stiffness matrix | 0.287 | 1.150 | 4.638 | |
| | DGM | solve the linear system by CG + AMG | 0.272 | 1.883 | 11.79 | |
| | | solve least squares problems | 0.113 | 0.463 | 1.861 | |
| | | assemble the stiffness matrix | 1.092 | 4.369 | 17.37 | |
| 3 | RDA | solve the linear system by CG + A_0^{-1} | 0.036 | 0.148 | 0.662 | |
| | | assemble the stiffness matrix | 0.568 | 2.280 | 9.576 | |
| | | solve the linear system by CG + AMG | 0.593 | 4.372 | 29.06 | |
| | 4 | RDA | solve least squares problems | 0.265 | 1.066 | 4.260 |
| | | | assemble the stiffness matrix | 2.392 | 9.301 | 37.23 |
| | | | solve the linear system by CG + A_0^{-1} | 0.077 | 0.324 | 1.546 |
| DGM | | assemble the stiffness matrix | 1.382 | 5.391 | 20.25 | |
| | | solve the linear system by CG + AMG | 1.723 | 12.29 | 67.29 | |
| | | solve least squares problems | 0.265 | 1.066 | 4.260 | |

TABLE 10. The CPU times for all steps in Example 4.

Example 5. In this example, we numerically solve the problem defined on $\Omega = (-1, 1)^2$ with a series of polygonal meshes. The polygonal meshes are generated by the package PolyMesher [40], which contain different types of polygon elements. The exact solution is

$$u(x, y) = e^{x^2+y^2} \sin(xy).$$

Because the polygonal meshes are not nested, only the algebraic multigrid method and the direct method are used to approximate A_0^{-1} . The numerical results are shown in Tab. 11 and Tab. 12. Clearly, the results demonstrate that the proposed method can work very well for elements of complex geometries and has a great efficiency on solving the linear system.

| m | Preconditioner θ | | $1/h$ | | | | | $1/h$ | | | | |
|-----|----------------------------|--------------|---------------|-----|------|------|------|-----------------|-----|------|------|-----|
| | | | 10 | 20 | 40 | 80 | 160 | 10 | 20 | 40 | 80 | 160 |
| | | | -1: symmetric | | | | | 1: nonsymmetric | | | | |
| 1 | A_0^{-1} | BoomerAMG | 24 | 27 | 29 | 30 | 31 | 19 | 20 | 21 | 21 | 21 |
| | | DirectSolver | 23 | 26 | 28 | 28 | 29 | 19 | 20 | 21 | 21 | 21 |
| | BoomerAMG | | 13 | 15 | 25 | 32 | 52 | 13 | 15 | 23 | 28 | 39 |
| | Identity | | 130 | 325 | 623 | 1230 | 2368 | 134 | 302 | 592 | 1406 | - |
| 2 | A_0^{-1} | BoomerAMG | 36 | 41 | 44 | 46 | 47 | 25 | 29 | 31 | 31 | 31 |
| | | DirectSolver | 36 | 40 | 43 | 44 | 44 | 26 | 29 | 31 | 31 | 31 |
| | BoomerAMG | | 17 | 21 | 28 | 52 | 82 | 17 | 21 | 27 | 43 | 66 |
| | Identity | | 150 | 415 | 800 | 1608 | - | 148 | 446 | 825 | 1880 | - |
| 3 | A_0^{-1} | BoomerAMG | 57 | 64 | 69 | 74 | 75 | 33 | 37 | 40 | 40 | 41 |
| | | DirectSolver | 56 | 63 | 67 | 71 | 71 | 33 | 37 | 41 | 40 | 41 |
| | BoomerAMG | | 33 | 42 | 49 | 62 | 98 | 32 | 39 | 46 | 59 | 74 |
| | Identity | | 228 | 614 | 1213 | 2509 | - | 180 | 543 | 1110 | 2793 | - |
| 4 | A_0^{-1} | BoomerAMG | 76 | 91 | 101 | 116 | 119 | 38 | 44 | 53 | 57 | 59 |
| | | DirectSolver | 75 | 89 | 99 | 111 | 113 | 39 | 44 | 53 | 57 | 59 |
| | BoomerAMG | | 62 | 75 | 95 | 116 | 156 | 55 | 72 | 89 | 105 | 129 |
| | Identity | | 308 | 977 | 2168 | - | - | 186 | 787 | 1702 | - | - |

TABLE 11. The convergence steps for symmetric and nonsymmetric methods in Example 5.

| m | Preconditioner θ | | $1/h$ | | | | | $1/h$ | | | | |
|-----|----------------------------|--------------|--------------|-------|-------|-------|-------|----------------|-------|-------|-------|-------|
| | | | 10 | 20 | 40 | 80 | 160 | 10 | 20 | 40 | 80 | 160 |
| | | | -1:symmetric | | | | | 1:nonsymmetric | | | | |
| 1 | A_0^{-1} | BoomerAMG | 0.002 | 0.009 | 0.033 | 0.131 | 0.555 | 0.002 | 0.006 | 0.022 | 0.099 | 0.466 |
| | | DirectSolver | 0.001 | 0.003 | 0.014 | 0.067 | 0.516 | 0.001 | 0.002 | 0.010 | 0.047 | 0.317 |
| | BoomerAMG | | 0.002 | 0.008 | 0.051 | 0.280 | 1.861 | 0.003 | 0.011 | 0.056 | 0.227 | 1.682 |
| | Identity | | 0.003 | 0.023 | 0.170 | 1.401 | 13.01 | 0.004 | 0.036 | 0.288 | 2.979 | - |
| 2 | A_0^{-1} | BoomerAMG | 0.003 | 0.016 | 0.052 | 0.239 | 1.197 | 0.003 | 0.010 | 0.038 | 0.151 | 0.709 |
| | | DirectSolver | 0.003 | 0.008 | 0.032 | 0.151 | 0.979 | 0.001 | 0.004 | 0.018 | 0.082 | 0.555 |
| | BoomerAMG | | 0.003 | 0.016 | 0.087 | 0.602 | 5.321 | 0.005 | 0.018 | 0.087 | 0.560 | 4.171 |
| | Identity | | 0.004 | 0.049 | 0.396 | 3.388 | - | 0.005 | 0.061 | 0.502 | 5.734 | - |
| 3 | A_0^{-1} | BoomerAMG | 0.005 | 0.023 | 0.090 | 0.403 | 1.793 | 0.003 | 0.012 | 0.045 | 0.187 | 0.825 |
| | | DirectSolver | 0.002 | 0.013 | 0.059 | 0.304 | 1.789 | 0.002 | 0.006 | 0.026 | 0.132 | 0.836 |
| | BoomerAMG | | 0.007 | 0.033 | 0.174 | 0.988 | 7.758 | 0.007 | 0.034 | 0.169 | 0.912 | 6.984 |
| | Identity | | 0.009 | 0.096 | 0.796 | 6.940 | - | 0.007 | 0.087 | 0.769 | 8.809 | - |
| 4 | A_0^{-1} | BoomerAMG | 0.007 | 0.035 | 0.155 | 0.779 | 3.911 | 0.004 | 0.015 | 0.066 | 0.330 | 1.674 |
| | | DirectSolver | 0.005 | 0.024 | 0.129 | 0.769 | 4.888 | 0.002 | 0.010 | 0.046 | 0.273 | 1.774 |
| | BoomerAMG | | 0.015 | 0.084 | 0.428 | 2.651 | 19.66 | 0.014 | 0.082 | 0.432 | 2.406 | 15.66 |
| | Identity | | 0.014 | 0.226 | 2.149 | - | - | 0.008 | 0.149 | 1.490 | - | - |

TABLE 12. The CPU times of solving linear system for symmetric and nonsymmetric methods in Example 5.

Example 6. In this case, we test an elliptic problem on the domain $\Omega = (-1, 1)^2$ with the coefficient matrix

$$A = \begin{pmatrix} 3 & 0 \\ 0 & 0.1 \end{pmatrix},$$

and the exact solution is selected by

$$u(x, y) = \sin\left(\frac{1}{3}x\right) + \cos(10y).$$

In this test, the penalty parameter in the symmetric scheme is taken as $\mu = 6m^2 + 10$. For such a problem, the convergence steps and CPU time of solving the final linear systems are recorded in Tab. 13 and Tab. 14, respectively. The preconditioned methods still have a good numerical performance for both symmetric and nonsymmetric interior penalty methods.

Example 7. We solve a three-dimensional elliptic problem defined in the cubic domain $\Omega = (0, 1)^3$. The exact solution is selected to be the same as Example 2. This problem is solved on a series of tetrahedral meshes with the mesh size $h = 1/4, 1/8, 1/16, 1/32$. The numerical results are reported in Tab. 15. In three dimensions, the proposed preconditioning method still has a fast convergence speed, and the

| m | Preconditioner θ | | $1/h$ | | | | | $1/h$ | | | | |
|-----|----------------------------|--------------|-------|------|------|------|-----|-------|------|------|------|-----|
| | | | 10 | 20 | 40 | 80 | 160 | 10 | 20 | 40 | 80 | 160 |
| 1 | A_0^{-1} | GMG | 36 | 46 | 52 | 57 | 59 | 40 | 48 | 57 | 62 | 66 |
| | | BoomerAMG | 37 | 46 | 54 | 58 | 60 | 41 | 48 | 56 | 60 | 64 |
| | | DirectSolver | 36 | 44 | 52 | 56 | 60 | 39 | 47 | 54 | 59 | 62 |
| | | BoomerAMG | 15 | 24 | 34 | 46 | 66 | 16 | 19 | 28 | 43 | 69 |
| | | Identity | 238 | 537 | 1036 | 2049 | - | 280 | 570 | 1098 | 2548 | - |
| 2 | A_0^{-1} | GMG | 62 | 79 | 88 | 92 | 97 | 68 | 81 | 89 | 93 | 96 |
| | | BoomerAMG | 61 | 78 | 89 | 95 | 100 | 66 | 84 | 92 | 97 | 98 |
| | | DirectSolver | 57 | 76 | 86 | 93 | 96 | 63 | 82 | 89 | 93 | 94 |
| | | BoomerAMG | 39 | 55 | 67 | 92 | 126 | 36 | 48 | 55 | 67 | 90 |
| | | Identity | 338 | 691 | 1412 | 2758 | - | 297 | 711 | 1613 | - | - |
| 3 | A_0^{-1} | GMG | 98 | 115 | 122 | 129 | 131 | 99 | 118 | 125 | 129 | 129 |
| | | BoomerAMG | 98 | 116 | 127 | 133 | 136 | 106 | 121 | 131 | 133 | 133 |
| | | DirectSolver | 94 | 113 | 123 | 129 | 131 | 102 | 117 | 126 | 129 | 129 |
| | | BoomerAMG | 44 | 65 | 78 | 99 | 130 | 46 | 62 | 70 | 82 | 105 |
| | | Identity | 437 | 905 | 1786 | - | - | 390 | 942 | 2229 | - | - |
| 4 | A_0^{-1} | GMG | 142 | 178 | 187 | 199 | 204 | 129 | 166 | 184 | 200 | 206 |
| | | BoomerAMG | 122 | 161 | 183 | 197 | 203 | 131 | 168 | 191 | 205 | 210 |
| | | DirectSolver | 122 | 157 | 176 | 192 | 198 | 129 | 163 | 186 | 200 | 208 |
| | | BoomerAMG | 99 | 171 | 211 | 239 | 273 | 72 | 132 | 161 | 181 | 209 |
| | | Identity | 577 | 1301 | 2584 | - | - | 469 | 1062 | - | - | - |

TABLE 13. The convergence steps for symmetric and nonsymmetric methods in Example 6.

| m | Preconditioner θ | | $1/h$ | | | | | $1/h$ | | | | |
|-----|----------------------------|--------------|-------|-------|-------|-------|--------|-------|-------|-------|-------|-------|
| | | | 10 | 20 | 40 | 80 | 160 | 10 | 20 | 40 | 80 | 160 |
| 1 | A_0^{-1} | GMG | 0.006 | 0.028 | 0.128 | 0.689 | 2.736 | 0.028 | 0.046 | 0.148 | 0.653 | 2.969 |
| | | BoomerAMG | 0.010 | 0.046 | 0.200 | 0.913 | 3.812 | 0.011 | 0.042 | 0.213 | 0.925 | 3.992 |
| | | DirectSolver | 0.004 | 0.025 | 0.130 | 0.926 | 6.034 | 0.005 | 0.023 | 0.118 | 1.007 | 5.974 |
| | | BoomerAMG | 0.011 | 0.060 | 0.284 | 1.777 | 11.39 | 0.013 | 0.052 | 0.271 | 1.837 | 12.81 |
| | | Identity | 0.020 | 0.183 | 1.408 | 15.19 | - | 0.038 | 0.322 | 2.665 | 35.41 | - |
| 2 | A_0^{-1} | GMG | 0.011 | 0.053 | 0.242 | 1.172 | 4.993 | 0.044 | 0.084 | 0.266 | 1.173 | 5.093 |
| | | BoomerAMG | 0.020 | 0.078 | 0.360 | 1.597 | 7.221 | 0.018 | 0.084 | 0.387 | 1.639 | 7.562 |
| | | DirectSolver | 0.009 | 0.047 | 0.245 | 1.692 | 10.20 | 0.009 | 0.047 | 0.236 | 1.943 | 12.32 |
| | | BoomerAMG | 0.027 | 0.152 | 0.721 | 4.698 | 22.56 | 0.030 | 0.155 | 0.706 | 4.154 | 20.40 |
| | | Identity | 0.035 | 0.281 | 2.378 | 18.93 | - | 0.066 | 0.417 | 4.343 | - | - |
| 3 | A_0^{-1} | GMG | 0.024 | 0.111 | 0.486 | 2.303 | 10.59 | 0.059 | 0.143 | 0.488 | 2.403 | 10.64 |
| | | BoomerAMG | 0.036 | 0.147 | 0.639 | 3.004 | 13.11 | 0.031 | 0.117 | 0.690 | 2.912 | 13.71 |
| | | DirectSolver | 0.020 | 0.103 | 0.514 | 3.826 | 15.56 | 0.018 | 0.083 | 0.436 | 3.769 | 15.20 |
| | | BoomerAMG | 0.041 | 0.217 | 1.074 | 7.294 | 41.81 | 0.042 | 0.199 | 0.960 | 5.696 | 36.81 |
| | | Identity | 0.072 | 0.618 | 5.140 | - | - | 0.065 | 0.705 | 7.763 | - | - |
| 4 | A_0^{-1} | GMG | 0.041 | 0.221 | 1.010 | 5.302 | 21.28 | 0.081 | 0.237 | 0.909 | 4.934 | 21.35 |
| | | BoomerAMG | 0.055 | 0.277 | 1.413 | 6.208 | 24.41 | 0.044 | 0.215 | 1.085 | 5.520 | 31.75 |
| | | DirectSolver | 0.033 | 0.185 | 1.012 | 6.038 | 27.45 | 0.026 | 0.143 | 0.866 | 5.854 | 27.10 |
| | | BoomerAMG | 0.109 | 0.788 | 4.583 | 25.08 | 115.20 | 0.089 | 0.703 | 3.865 | 20.66 | 89.13 |
| | | Identity | 0.133 | 1.264 | 10.66 | - | - | 0.092 | 0.956 | - | - | - |

TABLE 14. The CPU times of solving linear system for symmetric and nonsymmetric methods in Example 6.

convergence steps for symmetric/nonsymmetric systems keep almost unchanged as h tends to zero. This numerical observation validates the estimates in Theorem 3. The convergence histories for all accuracy $1 \leq m \leq 3$ are plotted in Fig. 4. The relative errors in iterations decrease sharply for our method. The CPU times costed in solving linear systems are displayed in Tab. 16. Clearly, our method is still efficient for problems in three dimensions.

| m | Preconditioner | | $1/h$ | | | | $1/h$ | | | |
|-----|----------------|--------------|--------------|-----|------|------|----------------|-----|------|------|
| | | | 4 | 8 | 16 | 32 | 4 | 8 | 16 | 32 |
| | θ | | -1:symmetric | | | | 1:nonsymmetric | | | |
| 1 | A_0^{-1} | GMG | 18 | 26 | 32 | 35 | 23 | 27 | 29 | 30 |
| | | BoomerAMG | 18 | 25 | 32 | 36 | 23 | 26 | 28 | 28 |
| | | DirectSolver | 17 | 24 | 31 | 34 | 23 | 26 | 27 | 28 |
| | | BoomerAMG | 9 | 15 | 26 | 36 | 8 | 13 | 23 | 33 |
| | | Identity | 155 | 399 | 788 | 1576 | 75 | 183 | 423 | 1333 |
| 2 | A_0^{-1} | GMG | 36 | 46 | 49 | 52 | 40 | 44 | 46 | 47 |
| | | BoomerAMG | 36 | 46 | 48 | 51 | 40 | 43 | 43 | 44 |
| | | DirectSolver | 36 | 45 | 46 | 50 | 40 | 43 | 44 | 44 |
| | | BoomerAMG | 18 | 28 | 42 | 66 | 18 | 26 | 40 | 62 |
| | | Identity | 186 | 522 | 1044 | 2047 | 160 | 493 | 1093 | 2460 |
| 3 | A_0^{-1} | GMG | 61 | 89 | 93 | 96 | 48 | 57 | 64 | 67 |
| | | BoomerAMG | 61 | 81 | 90 | 95 | 47 | 55 | 61 | 62 |
| | | DirectSolver | 61 | 80 | 88 | 93 | 48 | 56 | 61 | 63 |
| | | BoomerAMG | 43 | 64 | 75 | 92 | 46 | 69 | 76 | 88 |
| | | Identity | 277 | 812 | 1564 | - | 201 | 684 | 1417 | - |

TABLE 15. The convergence steps for symmetric and nonsymmetric methods in Example 7.

| m | Preconditioner | | $1/h$ | | | | $1/h$ | | | |
|-----|----------------|--------------|--------------|-------|-------|--------|----------------|-------|-------|--------|
| | | | 4 | 8 | 16 | 32 | 4 | 8 | 16 | 32 |
| | θ | | -1:symmetric | | | | 1:nonsymmetric | | | |
| 1 | A_0^{-1} | GMG | 0.003 | 0.022 | 0.218 | 2.092 | 0.003 | 0.018 | 0.202 | 1.969 |
| | | BoomerAMG | 0.003 | 0.038 | 0.500 | 6.832 | 0.004 | 0.026 | 0.306 | 4.045 |
| | | DirectSolver | 0.002 | 0.029 | 0.832 | 17.29 | 0.002 | 0.020 | 0.627 | 12.94 |
| | | BoomerAMG | 0.003 | 0.051 | 1.182 | 19.53 | 0.004 | 0.056 | 1.200 | 16.59 |
| | | Identity | 0.008 | 0.192 | 4.691 | 77.80 | 0.004 | 0.107 | 2.999 | 102.25 |
| 2 | A_0^{-1} | GMG | 0.007 | 0.067 | 0.659 | 5.684 | 0.006 | 0.038 | 0.424 | 4.029 |
| | | BoomerAMG | 0.010 | 0.089 | 0.969 | 8.216 | 0.009 | 0.069 | 0.825 | 7.336 |
| | | DirectSolver | 0.005 | 0.070 | 1.553 | 25.31 | 0.004 | 0.040 | 1.001 | 22.94 |
| | | BoomerAMG | 0.010 | 0.165 | 3.288 | 53.99 | 0.009 | 0.175 | 3.207 | 47.28 |
| | | Identity | 0.018 | 0.529 | 10.88 | 141.10 | 0.013 | 0.379 | 9.446 | 238.85 |
| 3 | A_0^{-1} | GMG | 0.022 | 0.220 | 2.837 | 23.39 | 0.019 | 0.165 | 1.705 | 16.52 |
| | | BoomerAMG | 0.018 | 0.241 | 2.742 | 30.52 | 0.015 | 0.185 | 1.826 | 21.15 |
| | | DirectSolver | 0.014 | 0.198 | 3.603 | 62.84 | 0.009 | 0.135 | 1.985 | 36.04 |
| | | BoomerAMG | 0.035 | 0.750 | 12.54 | 139.98 | 0.039 | 0.861 | 12.22 | 121.88 |
| | | Identity | 0.050 | 1.709 | 42.10 | - | 0.027 | 1.057 | 21.84 | - |

TABLE 16. The CPU times for symmetric and nonsymmetric methods in Example 7.

6. CONCLUSIONS

In this paper, we proposed a preconditioned interior penalty method for the elliptic problem with the reconstructed discontinuous approximation. The schemes are derived under the symmetric/nonsymmetric interior penalty DG methods. We constructed a preconditioner from the piecewise constant function and the preconditioned system is shown to be optimal. Numerical experiments demonstrated the efficiency on both the approximation by the reconstructed space and the iterative method for the preconditioned system.

ACKNOWLEDGEMENTS

The authors would like to thank the anonymous referees sincerely for their constructive comments that improve the quality of this paper. This research was supported by National Natural Science Foundation of China (12201442, 12288101).

DATA AVAILABILITY

The author declares that all data supporting the findings of this study are available within this particle.

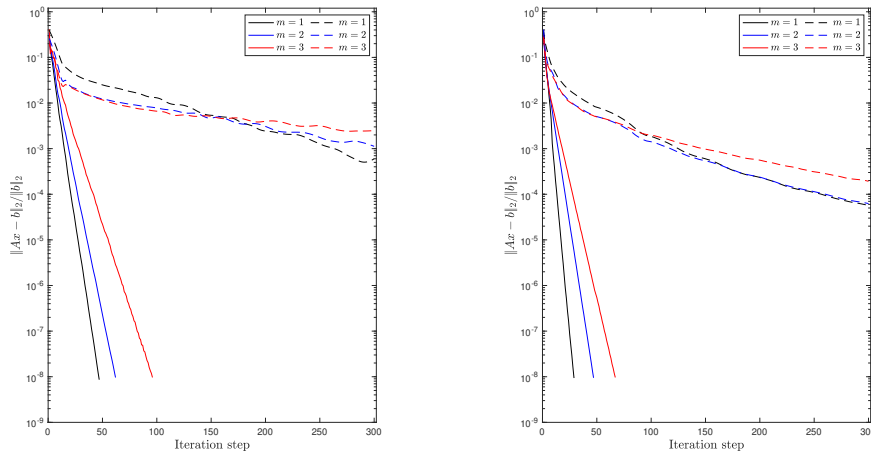


FIGURE 4. The convergence histories of CG (left) /GMRES (right) solvers on the mesh $h = 1/32$ (solid line: CG/GMRES solver with preconditioner A_0^{-1} , dashed line: standard CG/GMRES solver).

DECLARATIONS

The author has no relevant financial or non-financial interests to disclose.

REFERENCES

1. P. F. Antonietti and B. Ayuso, *Schwarz domain decomposition preconditioners for discontinuous Galerkin approximations of elliptic problems: non-overlapping case*, M2AN Math. Model. Numer. Anal. **41** (2007), no. 1, 21–54.
2. P. F. Antonietti, S. Giani, and P. Houston, *Domain decomposition preconditioners for discontinuous Galerkin methods for elliptic problems on complicated domains*, J. Sci. Comput. **60** (2014), no. 1, 203–227.
3. P. F. Antonietti and P. Houston, *A class of domain decomposition preconditioners for hp-discontinuous Galerkin finite element methods*, J. Sci. Comput. **46** (2011), no. 1, 124–149.
4. P. F. Antonietti, P. Houston, X. Hu, M. Sarti, and M. Verani, *Multigrid algorithms for hp-version interior penalty discontinuous Galerkin methods on polygonal and polyhedral meshes*, Calcolo **54** (2017), no. 4, 1169–1198.
5. P. F. Antonietti and L. Melas, *Algebraic multigrid schemes for high-order nodal discontinuous Galerkin methods*, SIAM J. Sci. Comput. **42** (2020), no. 2, A1147–A1173.
6. P. F. Antonietti, M. Sarti, M. Verani, and L. T. Zikatanov, *A uniform additive Schwarz preconditioner for high-order discontinuous Galerkin approximations of elliptic problems*, J. Sci. Comput. **70** (2017), no. 2, 608–630.
7. D. N. Arnold, *An interior penalty finite element method with discontinuous elements*, SIAM J. Numer. Anal. **19** (1982), no. 4, 742–760.
8. D. N. Arnold, F. Brezzi, B. Cockburn, and L. D. Marini, *Unified analysis of discontinuous Galerkin methods for elliptic problems*, SIAM J. Numer. Anal. **39** (2001/02), no. 5, 1749–1779.
9. A. T. Barker, S. C. Brenner, and L.-Y. Sung, *Overlapping Schwarz domain decomposition preconditioners for the local discontinuous Galerkin method for elliptic problems*, J. Numer. Math. **19** (2011), no. 3, 165–187.
10. L. Beirão da Veiga, K. Lipnikov, and G. Manzini, *The Mimetic Finite Difference Method for Elliptic Problems*, MS&A. Modeling, Simulation and Applications, vol. 11, Springer, Cham, 2014.
11. S. C. Brenner, J. Cui, T. Gudi, and L.-Y. Sung, *Multigrid algorithms for symmetric discontinuous Galerkin methods on graded meshes*, Numer. Math. **119** (2011), no. 1, 21–47.
12. K. Brix, M. Campos P., and W. Dahmen, *A multilevel preconditioner for the interior penalty discontinuous Galerkin method*, SIAM J. Numer. Anal. **46** (2008), no. 5, 2742–2768.
13. A. Cangiani, Z. Dong, E. H. Georgoulis, and P. Houston, *hp-version discontinuous Galerkin methods on polygonal and polyhedral meshes*, SpringerBriefs in Mathematics, Springer, Cham, 2017.
14. A. Cangiani, E. H. Georgoulis, and P. Houston, *hp-version discontinuous Galerkin methods on polygonal and polyhedral meshes*, Math. Models Methods Appl. Sci. **24** (2014), no. 10, 2009–2041.
15. P. Castillo, *Performance of discontinuous Galerkin methods for elliptic PDEs*, SIAM J. Sci. Comput. **24** (2002), no. 2, 524–547.
16. N. Chalmers and T. Warburton, *Low-order preconditioning of high-order triangular finite elements*, SIAM J. Sci. Comput. **40** (2018), no. 6, A4040–A4059.
17. B. Cockburn, G. E. Karniadakis, and C. W. Shu, *The development of discontinuous Galerkin methods*, Discontinuous Galerkin methods (Newport, RI, 1999), Lect. Notes Comput. Sci. Eng., vol. 11, Springer, Berlin, 2000, pp. 3–50.
18. V. A. Dobrev, R. D. Lazarov, P. S. Vassilevski, and L. T. Zikatanov, *Two-level preconditioning of discontinuous Galerkin approximations of second-order elliptic equations*, Numer. Linear Algebra Appl. **13** (2006), no. 9, 753–770.
19. M. Dryja, J. Galvis, and M. Sarkis, *BDDC methods for discontinuous Galerkin discretization of elliptic problems*, J. Complexity **23** (2007), no. 4–6, 715–739.

20. ———, *Balancing domain decomposition methods for discontinuous Galerkin discretization*, Domain decomposition methods in science and engineering XVII, Lect. Notes Comput. Sci. Eng., vol. 60, Springer, Berlin, 2008, pp. 271–278.
21. Y. Epshteyn and B. Rivière, *Estimation of penalty parameters for symmetric interior penalty Galerkin methods*, J. Comput. Appl. Math. **206** (2007), no. 2, 843–872.
22. R. D. Falgout, J. E. Jones, and U. M. Yang, *The design and implementation of hypre, a library of parallel high performance preconditioners*, Numerical solution of partial differential equations on parallel computers, Lect. Notes Comput. Sci. Eng., vol. 51, Springer, Berlin, 2006, pp. 267–294.
23. X. Feng and O. A. Karakashian, *Two-level additive Schwarz methods for a discontinuous Galerkin approximation of second order elliptic problems*, SIAM J. Numer. Anal. **39** (2001), no. 4, 1343–1365.
24. J. Gopalakrishnan and G. Kanschat, *A multilevel discontinuous Galerkin method*, Numer. Math. **95** (2003), no. 3, 527–550.
25. T. J. R. Hughes, G. Engel, L. Mazzei, and M. G. Larson, *A comparison of discontinuous and continuous Galerkin methods based on error estimates, conservation, robustness and efficiency*, Discontinuous Galerkin methods (Newport, RI, 1999), Lect. Notes Comput. Sci. Eng., vol. 11, Springer, Berlin, 2000, pp. 135–146.
26. O. Karakashian and C. Collins, *Two-level additive Schwarz methods for discontinuous Galerkin approximations of second-order elliptic problems*, IMA J. Numer. Anal. **37** (2017), no. 4, 1800–1830.
27. R. Li, Q. Liu, and F. Yang, *A reconstructed discontinuous approximation on unfitted meshes to $H(\text{curl})$ and $H(\text{div})$ interface problems*, Comput. Methods Appl. Mech. Engrg. **403** (2023), no. part A, Paper No. 115723, 27.
28. R. Li, P. Ming, Z. Sun, F. Yang, and Z. Yang, *A discontinuous Galerkin method by patch reconstruction for biharmonic problem*, J. Comput. Math. **37** (2019), no. 4, 563–580.
29. R. Li, P. Ming, Z. Sun, and Z. Yang, *An arbitrary-order discontinuous Galerkin method with one unknown per element*, J. Sci. Comput. **80** (2019), no. 1, 268–288.
30. R. Li, P. Ming, and F. Tang, *An efficient high order heterogeneous multiscale method for elliptic problems*, Multiscale Model. Simul. **10** (2012), no. 1, 259–283.
31. R. Li, Z. Sun, and F. Yang, *Solving eigenvalue problems in a discontinuous approximate space by patch reconstruction*, SIAM J. Sci. Comput. **41** (2019), no. 5, A3381–A3400.
32. R. Li and F. Yang, *A discontinuous Galerkin method by patch reconstruction for elliptic interface problem on unfitted mesh*, SIAM J. Sci. Comput. **42** (2020), no. 2, A1428–A1457.
33. ———, *A least squares method for linear elasticity using a patch reconstructed space*, Comput. Methods Appl. Mech. Engrg. **363** (2020), no. 1, 112902.
34. K. Lipnikov, D. Vassilev, and I. Yotov, *Discontinuous Galerkin and mimetic finite difference methods for coupled Stokes-Darcy flows on polygonal and polyhedral grids*, Numer. Math. **126** (2013), 1–40.
35. L. Olson and J. B. Schroder, *Smoothed aggregation multigrid solvers for high-order discontinuous Galerkin methods for elliptic problems*, J. Comput. Phys. **230** (2011), no. 18, 6959–6976.
36. W. Pazner, *Efficient low-order refined preconditioners for high-order matrix-free continuous and discontinuous Galerkin methods*, SIAM J. Sci. Comput. **42** (2020), no. 5, A3055–A3083.
37. W. Pazner, T. Kolev, and C. R. Dohrmann, *Low-order preconditioning for the high-order finite element de Rham complex*, SIAM J. Sci. Comput. **45** (2023), no. 2, A675–A702.
38. M. J. D. Powell, *Approximation theory and methods*, Cambridge University Press, Cambridge-New York, 1981.
39. B. Rivière, *Discontinuous Galerkin methods for solving elliptic and parabolic equations*, Frontiers in Applied Mathematics, vol. 35, Society for Industrial and Applied Mathematics (SIAM), Philadelphia, PA, 2008, Theory and implementation.
40. C. Talischi, G. H. Paulino, A. Pereira, and I. F. M. Menezes, *PolyMesher: a general-purpose mesh generator for polygonal elements written in Matlab*, Struct. Multidiscip. Optim. **45** (2012), no. 3, 309–328.
41. J. Xu, *Iterative methods by space decomposition and subspace correction*, SIAM Rev. **34** (1992), no. 4, 581–613.
42. J. Xu and X.-C. Cai, *A preconditioned GMRES method for nonsymmetric or indefinite problems*, Math. Comp. **59** (1992), no. 200, 311–319.
43. J. Xu and L. Zikatanov, *Algebraic multigrid methods*, Acta Numer. **26** (2017), 591–721.

CAPT, LMAM AND SCHOOL OF MATHEMATICAL SCIENCES, PEKING UNIVERSITY, BEIJING 100871, P.R. CHINA; CHONGQING RESEARCH INSTITUTE OF BIG DATA, PEKING UNIVERSITY, CHONGQING 401121, P.R. CHINA

Email address: rli@math.pku.edu.cn

SCHOOL OF MATHEMATICAL SCIENCES, PEKING UNIVERSITY, BEIJING 100871, P.R. CHINA

Email address: qcliu@pku.edu.cn

COLLEGE OF MATHEMATICS, SICHUAN UNIVERSITY, CHENGDU 610065, P.R. CHINA

Email address: yangfanyi@scu.edu.cn